



A EUROPEAN JOURNAL

# CHEMPHYSICHEM

OF CHEMICAL PHYSICS AND PHYSICAL CHEMISTRY

## Accepted Article

**Title:** Near infrared photoactive aza-BODIPY: thermally robust and photostable photosensitizer and efficient electron donor

**Authors:** Łukasz Łapok, Igor Cieślak, Tomasz Pędziński, Katarzyna M. Stadnicka, and Maria Nowakowska

This manuscript has been accepted after peer review and appears as an Accepted Article online prior to editing, proofing, and formal publication of the final Version of Record (VoR). This work is currently citable by using the Digital Object Identifier (DOI) given below. The VoR will be published online in Early View as soon as possible and may be different to this Accepted Article as a result of editing. Readers should obtain the VoR from the journal website shown below when it is published to ensure accuracy of information. The authors are responsible for the content of this Accepted Article.

**To be cited as:** *ChemPhysChem* 10.1002/cphc.202000117

**Link to VoR:** <http://dx.doi.org/10.1002/cphc.202000117>

WILEY-VCH

[www.chemphyschem.org](http://www.chemphyschem.org)



## Graphical abstract

## Near infrared photoactive aza-BODIPY: thermally robust and photostable photosensitizer and efficient electron donor

Dr. Łukasz Łapok<sup>1\*</sup>, Igor Cieślak<sup>1</sup>, Dr. Tomasz Pędziniński<sup>2,3</sup>, Prof. Dr. Katarzyna M. Stadnicka<sup>1</sup>,  
Prof. Dr. Maria Nowakowska<sup>1</sup>

<sup>1</sup>Faculty of Chemistry, Jagiellonian University, Gronostajowa 2, 30-387 Kraków, Poland.

<sup>2</sup>Faculty of Chemistry, Adam Mickiewicz University in Poznań, 89b Umultowska, 61-614 Poznań,  
Poland.

<sup>3</sup>Center for Advanced Technology, Adam Mickiewicz University in Poznań, 10, 61-614 Poznań, Poland

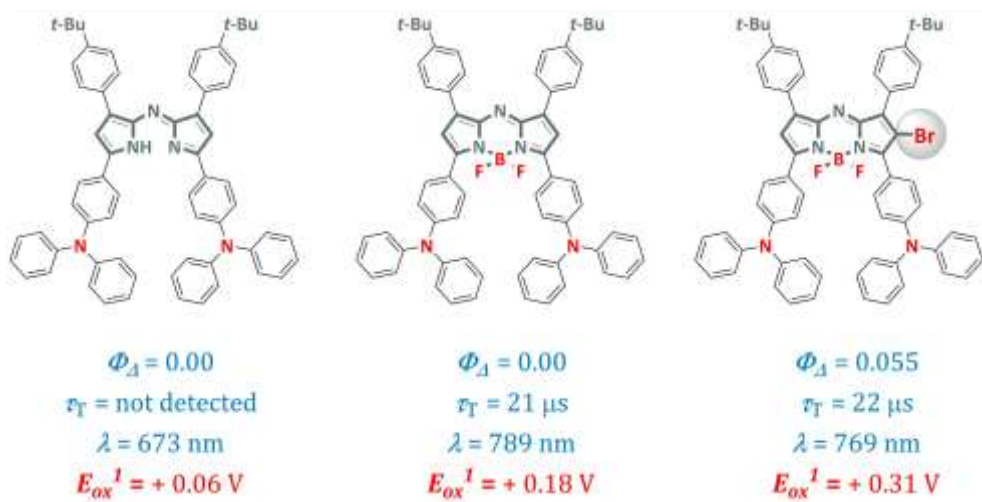


## Table-of-contents

### Abstract

- 1. Introduction**
- 2. Results and discussion**
  - 2.1. Synthesis and characterization*
  - 2.2. Optical properties*
  - 2.3. Time-resolved spectroscopy*
  - 2.4. Photosensitization*
  - 2.5. Electrochemistry and HOMO/LUMO energy levels*
  - 2.6. Photostability and thermal stability*
- 3. Discussion**
- 4. Experimental**
  - 4.1. Materials and methods*
  - 4.2. Synthesis*
- 5. Conclusions**
- 6. Acknowledgements**
- 7. References**

# Near infrared photoactive aza-BODIPY: thermally robust and photostable photosensitizer and efficient electron donor

Dr. Łukasz Łapok<sup>1\*</sup>, Igor Cieślak<sup>1</sup>, Dr. Tomasz Pędziński<sup>2,3</sup>, Prof. Dr. Katarzyna M. Stadnicka<sup>1</sup>,  
Prof. Dr. Maria Nowakowska<sup>1</sup>

<sup>1</sup>Faculty of Chemistry, Jagiellonian University, Gronostajowa 2, 30-387 Kraków, Poland.

<sup>2</sup>Faculty of Chemistry, Adam Mickiewicz University in Poznań, 89b Umultowska, 61-614 Poznań,  
Poland.

<sup>3</sup>Center for Advanced Technology, Adam Mickiewicz University in Poznań, 10, 61-614 Poznań, Poland

\*Corresponding author: [lukaszlapok@chemia.uj.edu.pl](mailto:lukaszlapok@chemia.uj.edu.pl), Tel.: +48 12 686 25 31, Fax: + 48 12 686 27 50.

**Keywords:** aza-BODIPY; triplet photosensitizer; excited-triplet state; near infrared absorption; photosensitization,

## Abstract

We report herein a synthesis of aza-BODIPY substituted with strongly electron-donating *p*-(diphenylamino)phenyl substituents (*p*-Ph<sub>2</sub>N-) at 3,5-positions. The presence of *p*-Ph<sub>2</sub>N-groups lowered the energy of the singlet excited state ( $E_s$ ) to 1.48 eV and induced NIR absorption with  $\lambda_{abs}$  at 789 nm in THF. The compound studied was weakly emissive with the emission band ( $\lambda_f$ ) at 837 nm and with the singlet lifetime ( $\tau_s$ ) equal 100 ps. Nanosecond laser photolysis experiments of aza-BODIPY in question revealed  $T_1 \rightarrow T_n$  absorption spanning from ca. 350 nm to ca. 550 nm with the triplet lifetime ( $\tau_T$ ) equal 21  $\mu$ s. By introducing a heavy atom (Br) into the structure of the aza-BODIPY we managed to turn it into a NIR operating photosensitizer. The photosensitized oxygenation of the model compound – diphenylisobenzofuran (DPBF) – proceeded via Type I and/or Type III mechanism without formation of singlet oxygen ( $^1O_2$ ). As estimated by CV/DPV measurements, the *p*-Ph<sub>2</sub>N-

substituted aza-BODIPYs studied exhibited oxidation processes at a relatively low oxidation potentials ( $E_{\text{ox}}^1$ ), pointing to the very good electron-donating properties of these molecules. Extremely high photostability and thermal robustness up to approximately 300°C were observed for the *p*-Ph<sub>2</sub>N- substituted aza-BODIPYs.

## 1. Introduction

Dyes active in the near-infrared part of the spectrum (700 – 1100 nm) are highly sought-after for both biomedical and high-tech applications [1,2]. Exemplarily, NIR active fluorophores are promising molecular probes for both *in vivo* and *in vitro* bioimaging [3-5]. The advantage of imaging in the NIR region stems from the fact that at wavelengths above 700 nm tissue autofluorescence is significantly reduced and tissue components such as hemoglobin and skin melanin exhibit negligible absorbance and scattering of near-infrared light. Furthermore, triplet sensitizers capable of absorbing near-infrared light are highly sought-after for biomedical applications - in particular for photodynamic therapy of cancer (PDT) [6,7]. It is well-established that the depth of light penetration into a tissue strongly depends on the light wavelength and it increases with the increase of the light wavelength. Exemplarily, light with a wavelength shorter than 550 nm is unsuitable for PDT, however, ability of light to penetrate tissue doubles from 550 nm to 650 nm and it doubles further as the wavelength shifts to 700 nm. Further increase of light wavelength from 700 nm to 800 nm results in an increase of the ability of light to penetrate tissue of 10 %. These empirical observations have some practical implications, viz. in order to treat more deeply seated tumors, triplet photosensitizers possessing long-wavelength absorption are needed. Consequently, the “therapeutic window” for PDT was defined as 600-1100 nm [8]. Typical NIR absorbing dyes are squarines [9], diketopyrrolopyrroles [10], some derivatives of porphyrins [11] and phthalocyanines [12], cyanines [13,14] and rylenes [15].

An interesting group of organic chromophores that have gained widespread attention in recent years as red/NIR active fluorophores and photosensitizers are aza-BODIPYs (aza-4,4-difluoro-4-bora-3*a*,4*a*-diazas-indacene) [16,17]. Structurally, aza-BODIPY dyes are derivatives of better known BODIPY dyes (4,4-difluoro-4-bora-3*a*,4*a*-diazas-indacene) obtained by replacing the meso-carbon atom that connects both pyrrole rings with an aza-

bridge [18-27]. Replacement of the meso-carbon atom with an aza-bridge results in a bathochromic shift of both absorption ( $\lambda_{\text{abs}}$ ) and emission ( $\lambda_{\text{fl}}$ ) bands of around 80 nm. Owing to their advantageous photophysical properties (triplet lifetimes  $\tau_{\text{T}}$ , triplet state quantum yields  $\Phi_{\text{T}}$  and triplet state energies  $E_{\text{T}}$ ) combined with tunable singlet oxygen quantum yields ( $\Phi_{\Delta}$ ) and ability to absorb light from the “therapeutic window”, aza-BODIPYs have been proposed as potential triplet photosensitizers for both *anti*-microbial and *anti*-cancer photodynamic therapy [18,28-49]. Furthermore, aza-BODIPYs were considered as fluorescent chemosensors for the detection of ammonia [50], cysteine, homocysteine and glutathione in living cells [51],  $\text{Hg}^{2+}$  [52-54],  $\text{F}^{-}$  [55,56], *in vivo* detection of  $\text{H}_2\text{S}$  and  $\text{NO}$  [57], carbon dioxide [58], glucose in whole blood [59] and pH-sensitive sensors [60]. Aza-BODIPYs have also been tested as photoactive components in photovoltaic devices [61-63] and nonlinear optical materials [64].

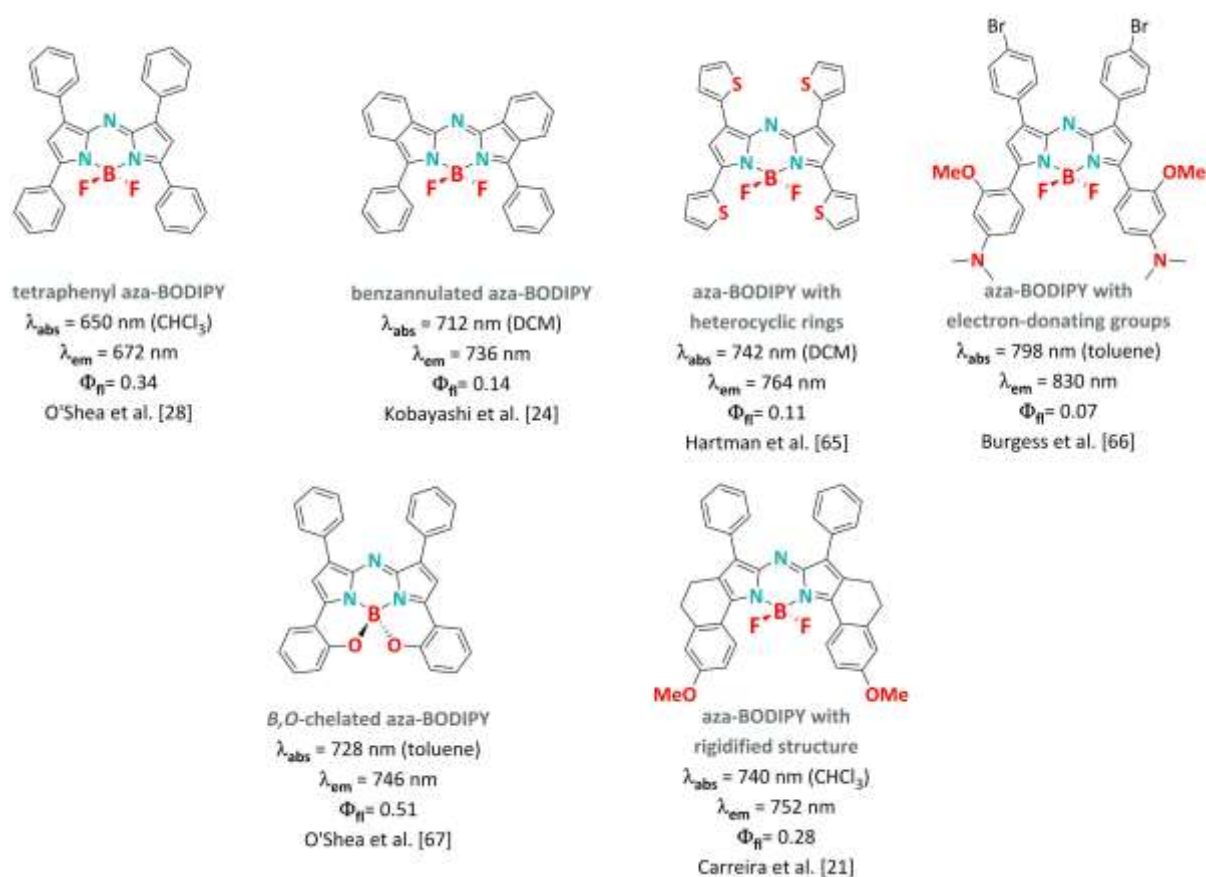


**Figure 1.** Strategies employed to induce near-infrared absorption and emission in aza-BODIPYs.

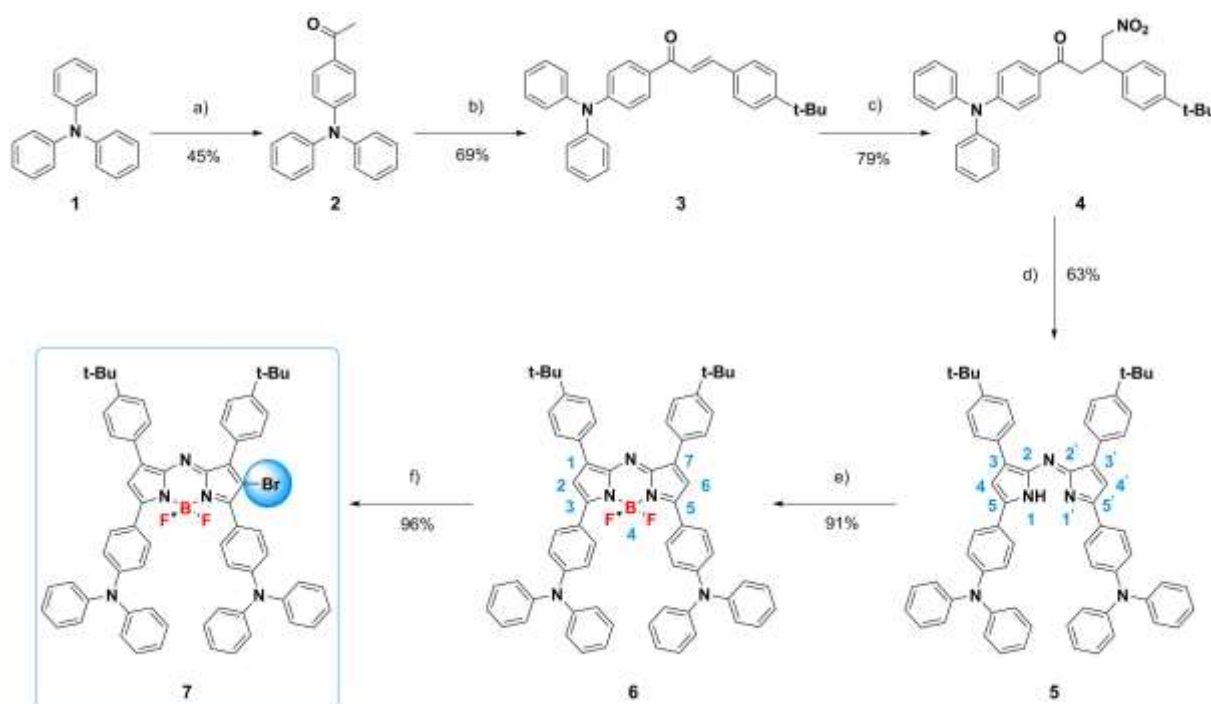
Typical strategies applied to induce near infrared light absorption in aza-BODIPYs include: a) functionalization of the chromophore with strong electron-donating groups, b) rigidification of the structure and c) extension of the  $\pi$ -electron system (fused aza-BODIPYs) (Figure 1) [21,24,28,65-67].

Our interest in efficient yet stable organic triplet photosensitizers capable of light absorption from the visible and near-IR part of the spectrum has led us to the discovery of novel aza-BODIPYs [68-72]. Herein, we report the five-steps synthesis and a comprehensive study on the photophysical and electrochemical properties of aza-BODIPY substituted with strongly electron-donating *p*-(diphenylamino)phenyl substituents (*p*-Ph<sub>2</sub>N) at 3,5-positions (see Scheme 1). It is well established that the presence of strong electron-donating substituents in the aza-BODIPY structure results in significant bathochromic shift of the absorption and emission bands. In an effort to induce highly desirable photophysical and photochemical properties important for biomedical applications we introduced a heavy atom – in this case bromine – into the structure of the aza-BODIPY in question. Empirical observations indicate that the presence of atoms with high atomic numbers (I, Br, Pt, Tl, Pb, etc.) induces a spin orbit coupling, facilitates intersystem crossing (ISC) and increases the population of molecules in their excited-triplet state ( $T_1$ ). In addition, the aza-BODIPY presented in this work was equipped with *p*-*tert*-butylphenyl rings at 1,7 positions to improve solubility and consequently facilitate purification and spectroscopic analysis. Understanding the relationship between the aza-BODIPY structure and the triplet state properties (such as triplet lifetime  $\tau_T$  and triplet state energy  $E_T$ ) is of paramount importance for developing next generation photosensitizers for biomedical applications, artificial light-harvesting systems, efficient photocatalysts as well as non-linear optical materials. This paper aims at exploring the possibility of triplet-state formation in aza-BODIPYs substituted with *p*-Ph<sub>2</sub>N groups by measuring the triplet-state lifetimes ( $\tau_T$ ) through recording the decay of the transient  $T_1 \rightarrow T_n$  absorption in nanosecond time-resolved transient absorption spectra. Furthermore, *via* electrochemical measurements (CV and DPV), we explored the redox properties ( $E_{ox}^1$ ,  $E_{red}^1$ ) and we estimated the alignment of the HOMO/LUMO energy levels of these novel aza-BODIPY derivatives. With the help of thin-layer spectroelectrochemical measurements we tried to shed some light on the relative stabilities of the electrochemically generated cation radicals (aza-BODIPY<sup>•+</sup>) and anion radicals (aza-BODIPY<sup>•-</sup>) – a property of prime importance

for evaluating the potential application of organic photoactive materials in organic electronics. Also, the solution photo-stability and thermal stability of these materials were evaluated.

## 2. Results and discussion

### 2.1. Synthesis and characterization



**Scheme 1.** Synthesis of mono-bromo aza-BODIPY **7**. Reaction conditions: a) acetyl chloride,  $\text{ZnCl}_2$ , DCM,  $0^\circ\text{C}$  to reflux, 24 h, 45%; b) 4-*tert*-butylbenzaldehyde, NaOH, EtOH,  $0^\circ\text{C}$  to RT, 24 h, 69%; c)  $\text{MeNO}_2$ ,  $\text{K}_2\text{CO}_3$ , MeOH, reflux, 17h, 79% ; d)  $\text{CH}_3\text{COONH}_4$ , n-butanol,  $117^\circ\text{C}$ , 3h, 63%; e)  $\text{BF}_3\cdot\text{Et}_2\text{O}$ , DIPA, DCM, 1h, 91%; f) NBS, DCM, 2h,  $0^\circ\text{C}$ , 96%.

The synthesis of aza-BODIPY under question is presented in Scheme 1. The synthesis started with the preparation of the precursor compound, i.e. 1-(4-(diphenylamino)phenyl)ethan-1-

one (**2**) [73]. Compound **2** was prepared by a Friedel-Crafts acylation of triphenylamine (**1**) in the presence of zinc chloride as a Lewis acid in 45 % yield. While optimizing the reaction conditions for **2** we tested several Lewis acids such as AlCl<sub>3</sub> and FeCl<sub>3</sub>, with ZnCl<sub>2</sub> giving the best results in terms of purity and the yield of the final product **2**. Also, acetyl chloride proved to be a better source of the acetyl group in comparison to acetic acid anhydride. The reaction of 4-*tert*-butylbenzaldehyde with ketone **2** in a base catalyzed aldol reaction led to a chalcone ( $\alpha,\beta$ -unsaturated ketone) **3** in 69 % yield. The nucleophilic addition of carbanion formed from nitromethane to the  $\alpha,\beta$ -unsaturated ketone **3** (Michael addition) resulted in formation of 1,3-diaryl-4-nitro-butan-1-one **4** in very good yield of 79 %. Despite numerous attempts we failed to get compound **4** in a pure form. Neither column chromatography nor crystallization or sublimation under vacuum allowed purification of **4**. We managed, however, to isolate a small amount of pure **4** with the help of a preparative thin layer chromatography (Figure S28). The sample obtained was used for the spectroscopic characterization of **4** and to calculate the reaction yield. The unpurified compound **4** was used, however, for the next reaction step. Refluxing of 1,3-diaryl-4-nitro-butan-1-one **4** in *n*-butanol in the presence of NH<sub>4</sub>OAc resulted in aza-dipyrromethene **5** (ADPM) in 63 % yield. Reaction of aza-dipyrromethene ligand **5** with an ethereal complex of boron trifluoride in dichloromethane and in the presence of diisopropylamine (DIPA), followed by chromatographic purification afforded the corresponding aza-BODIPY **6** in excellent yield of 91 %. The incorporation of boron into the ligand **5** was confirmed by <sup>11</sup>B and <sup>19</sup>F NMR spectroscopy. The <sup>11</sup>B resonance signal was found at  $\delta = 1.23$  ppm for **6** and it was seen as a triplet ( $^1J = 32.5$  Hz) pointing to the <sup>11</sup>B–<sup>19</sup>F interactions. The <sup>19</sup>F resonance signal was seen as a quartet at  $\delta = -111.01$  ppm due to the <sup>11</sup>B–<sup>19</sup>F interaction ( $^1J = 32.8$  Hz). In order to explore the impact of heavy halogen atoms on the excited triplet state characteristics of the aza-BODIPY **6** we looked at the possibility of introducing heavy atoms, such as iodine or bromine, into the structure of **6**. Our initial attempt to introduce iodine atoms into the structure of **6**, with *N*-iodosuccinimide (NIS) as the halogenating reagent, failed. Regardless of the reaction conditions applied (reaction temperatures ranging from -60°C to RT, different reaction times and solvents, different molar ratios of **6** to NIS) we observed either decomposition of the products or formation of an inseparable mixture of products with different degree of halogenation. Much better results were obtained when NIS was replaced with *N*-bromosuccinimide (NBS) in DCM as the source of bromonium cation Br<sup>+</sup>. However, the

precise control of the reaction outcome still proved to be extremely challenging. After numerous attempts with various reaction conditions we managed to regioselectively introduce one bromine atom per molecule of **6**. The ratio of NBS to aza-BODIPY **6** had to be kept strictly as 1:1 as any increase of the amount of NBS resulted in an inseparable mixture of products. The mono-bromo derivative **7** was isolated in 96% yield.

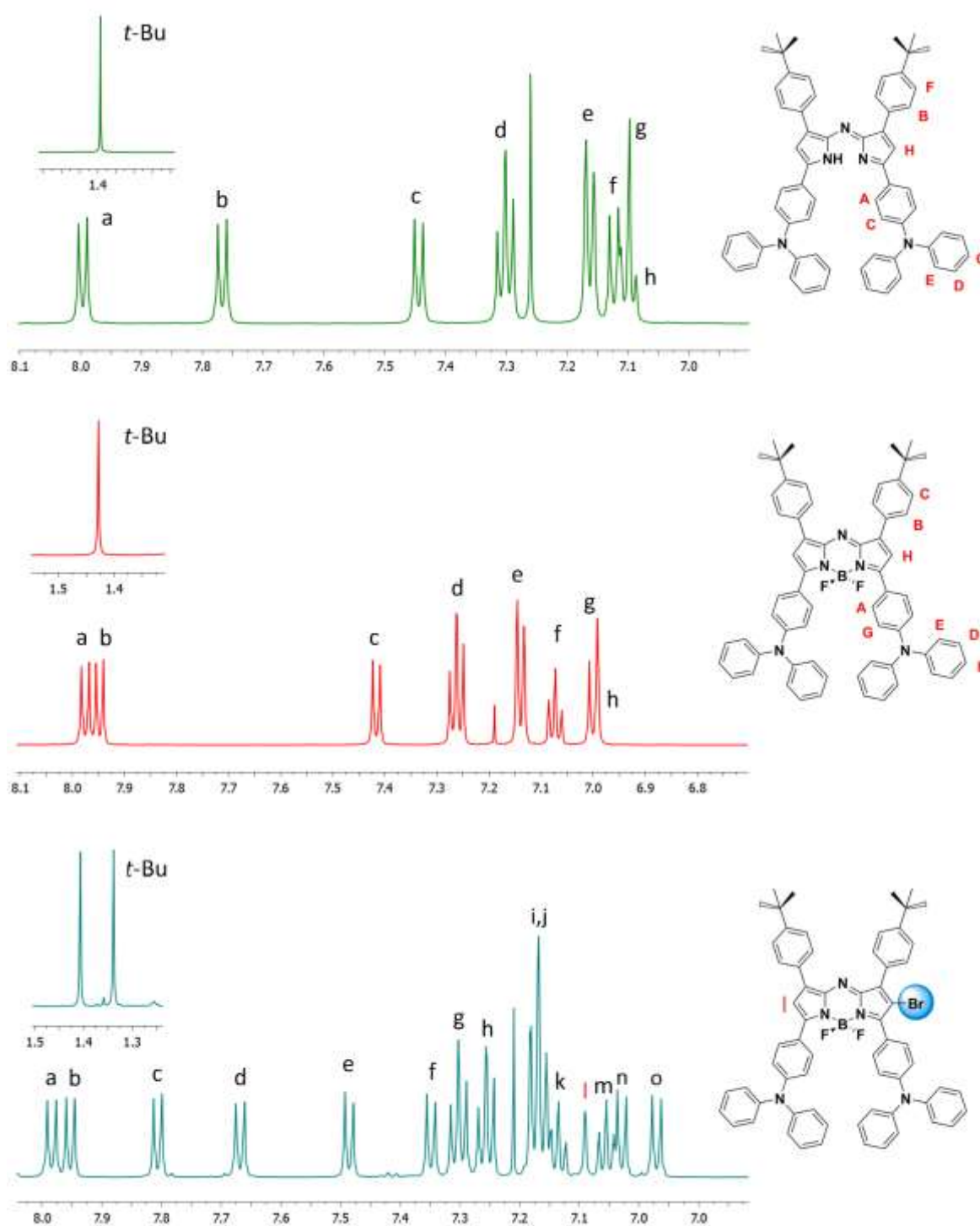


**Figure 2.**  $^1\text{H}$  NMR spectra of ADPM **5**, aza-BODIPYs **6** and its brominated derivative **7** in  $\text{CDCl}_3$ .

The regioselective introduction of bromine into the 2-position of the pyrrole ring was unambiguously confirmed by  $^1\text{H}$  NMR spectroscopy (see Figure 2 and Supporting Information). The  $^1\text{H}$  NMR spectrum of **7** is much more complex comparing to the  $^1\text{H}$  NMR spectrum of **6**, indicating the loss of symmetry for **7**. The diagnostic resonance of the pyrrole ring proton at 6-position was observed in the  $^1\text{H}$  NMR spectrum of **7** as a singlet at  $\delta = 7.14$  ppm with the integration equal precisely to one proton. Also, in the high resolution ESI spectrum a peak at  $m/z$  1023.3702 confirmed formation of mono-bromo derivative **7**. The identity of all intermediates, ADPM **5**, aza-BODIPY **6** and the mono-bromo derivative **7** presented in this work was supported by high resolution ESI mass spectrometry,  $^{11}\text{B}$  NMR,  $^{19}\text{F}$  NMR,  $^1\text{H}$  NMR,  $^{13}\text{C}$  NMR, FT-ATR-IR and elemental analysis (see Supporting Information), respectively.

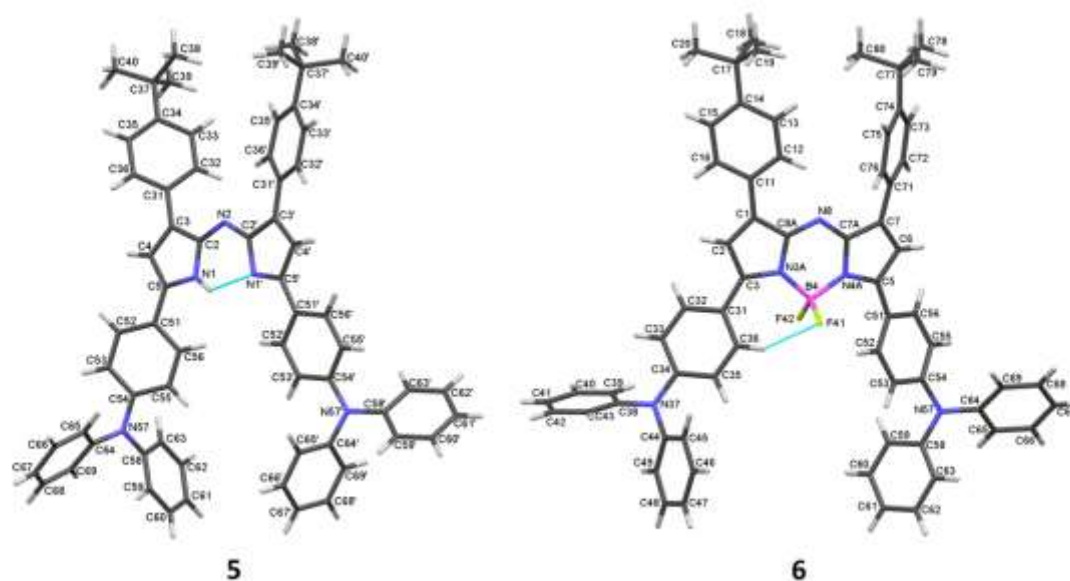


**Figure 3.** The conformation of the molecules ADPM **5** and aza-BODIPY **6** stabilized by intramolecular hydrogen bonds marked by dashed blue line along with the atom numbering scheme.

The structures of **5** and **6** were unambiguously confirmed by single crystal X-ray analysis (see Supporting Information and Figure 3). In turn, the mono-brominated derivative **7** did not

form crystals that could be subjected to X-ray analysis. The conformations of the molecules **5** and **6** with the atomic displacement ellipsoids for non-hydrogen atoms were shown in Figures S27 and S28, while the selected bond lengths, valence angles, torsion and dihedral angles were presented in Table S2. Crystal structures of compounds **5** and **6** follow the symmetry of space groups  $P-1$  and  $P21/c$ , respectively. The asymmetric unit of **5** contains the ADPM molecule and dichloromethane in the ratio of 1:0.694 (Figure S30). The nitrogen atoms **N(37)** and **N(57)** of ligand **5**, as well as the nitrogen atoms **N(57)** and **N(57')** of aza-BODIPY **6**, clearly show  $sp^2$  configuration (Figure 4).

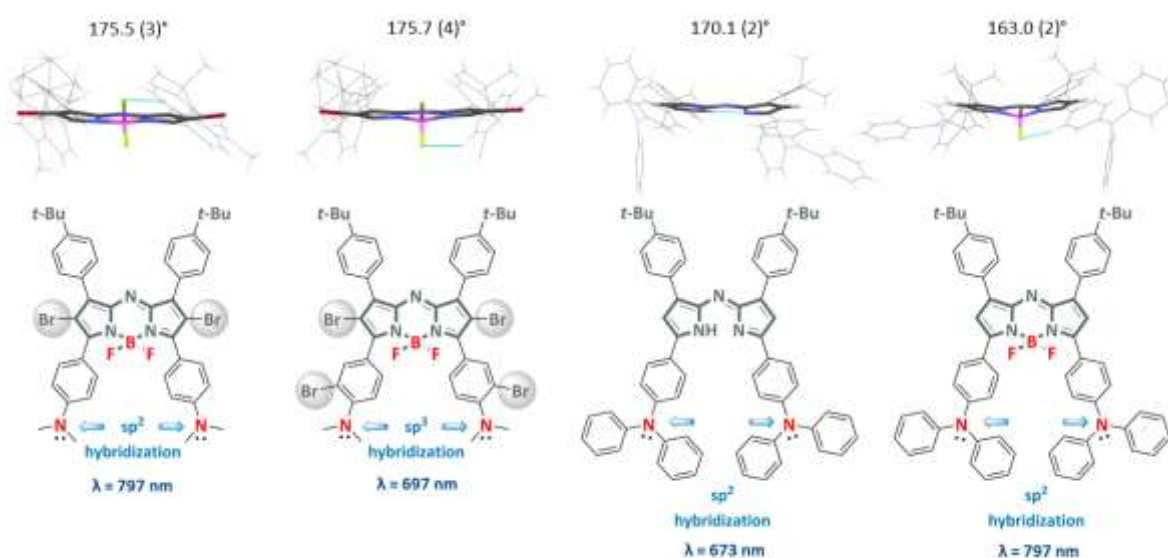


**Figure 4.** A comparison of the dihedral angles (top) between the five-membered rings of the central chromophore and the hybridizations of the nitrogen atoms of the amino groups for different ADPM and aza-BODIPYs substituted with either  $p$ -(Me<sub>2</sub>N) or  $p$ -(Ph<sub>2</sub>N) groups [71].

Interestingly, the chromophore moiety **C(1)C(2)C(3)N(3A)B(4)N(4A)C(5)C(6)C(7)C(7A)N(8)C(8A)** of **6** is not planar (the root mean square deviation, rms, of the fitted atoms from the best plane equals 0.1425 Å) (Figure 4). The observed deviation from planarity is due to tetrahedral configuration of boron atom of the BF<sub>2</sub> moiety (the average value of the valence angles at **B(4)** is equal to 109.4°). Only **N(3A)N(4A)C(7A)N(8)C(8A)** part of the central six-membered ring is planar (rms deviation of fitted atoms = 0.011 Å) and together with **B(4)** atom deviating from the best plane by 0.186(7) Å define a half-chair conformation of the **N(3A)B(4)N(4A)C(7A)N(8)C(8A)** six-

membered ring. The general conformation of both molecules is stabilized by intramolecular hydrogen bonds: **N(1)-H(1)...N(1')** in the case of **5** and **C(36)-H(36)...F(41)**, **C(52)-H(52)...F(41)** and **C(12)-H(12)...N(8)** in the case of **6**. The geometry of all intra- and intermolecular hydrogen bonds as well as the other selected weak interactions are given in Table S3. In Figure 4 we compared both the geometry of the central chromophore, viz. the dihedral angles formed between the adjacent pyrrole rings, the hybridization of the nitrogen atoms of the amino group and the optical properties ( $\lambda_{\text{abs}}$ ) of a set of aza-BODIPYs bearing *p*-aminophenyl substituents at 3,5-positions. The crystallographic data and the optical properties of two of the structures presented in Figure 4 were recently reported by us in our ChemPhysChem paper [71].

## 2.2. Optical properties

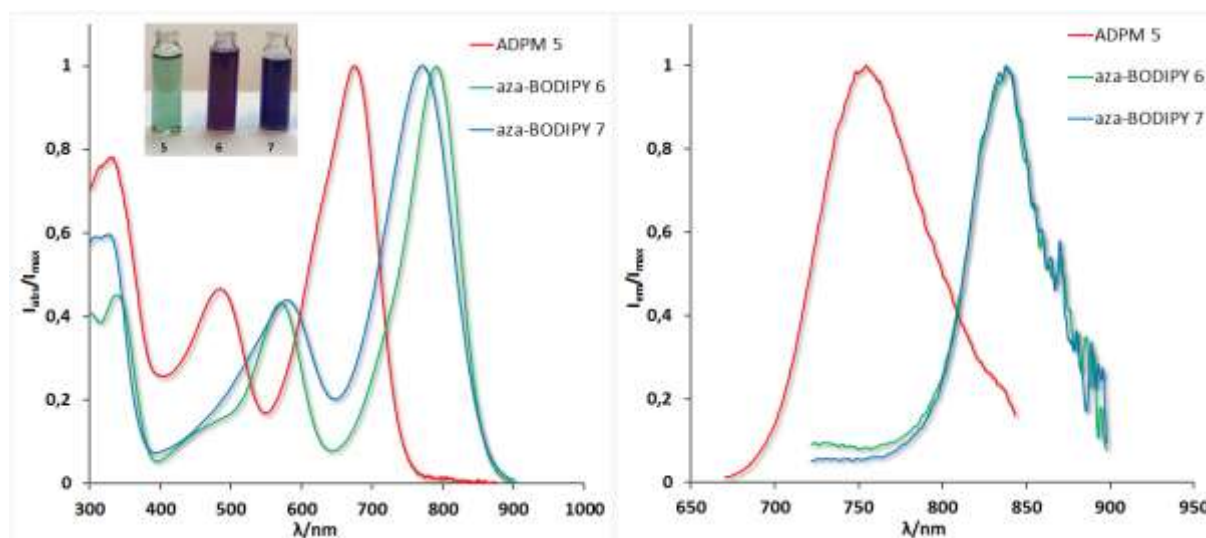


**Figure 5.** Normalized absorption (left panel) and normalized corrected emission (right panel) spectra of **5-7** in THF at room temperature (inset: THF solutions of compounds studied). Excitation wavelength:  $\lambda_{\text{ex}} = 650$  nm for **5**,  $\lambda_{\text{ex}} = 700$  nm for **6** and **7**.

The absorption and emission spectra of ADPM **5** and aza-BODIPYs **6** and **7** in THF are outlined in Figure 5 and summarized in Table 1. Compounds **5-7** share similar spectral

features, viz. an intense absorption band in the visible or near-IR part of the spectrum ( $S_0 \rightarrow S_1$ ), accompanied by another, blue-shifted, weaker absorption band ca. half the intensity of the main absorption band. This additional absorption band we attributed to the  $\pi\text{-}\pi^*$  transitions involving orbitals below the HOMO or above the LUMO. A similar spectral feature was observed for aza-BODIPY with dimethylamino groups ( $\text{Me}_2\text{N-}$ ) in *para*- position of the phenyl rings at 3,5-positions of the chromophore core (Figure 4) [71]. THF solutions of aza-dipyrrromethene **5** exhibit a bright green color with  $\lambda_{\text{abs}}$  equal 673 nm ( $\epsilon = 48\,000\text{ M}^{-1}\text{ cm}^{-1}$ ). Incorporation of difluoroboron into **5** resulted in a pronounced red-shift of the absorption band of 116 nm. The aza-BODIPY **6** absorbed light at  $\lambda_{\text{abs}}$  789 nm with a high molar absorption coefficient of  $\epsilon = 83\,000\text{ M}^{-1}\text{ cm}^{-1}$  and exhibited an intense reddish/violet color resulting from the additional absorption band at  $\lambda_{\text{abs}}$  570 nm.

Functionalization of aza-BODIPY **6** with bromine at 2-position of the pyrrole ring retained its ability to absorb light from the near-IR part of the spectrum. Monobromo-derivative **7** absorbed light at  $\lambda_{\text{abs}}$  769 nm with a molar absorption coefficient of  $\epsilon = 55\,000\text{ M}^{-1}\text{ cm}^{-1}$  and exhibited deep navy color.

**Table 1.** Summary of spectroscopic and photophysical data for compounds **5**, **6**, **7** and **8** in THF.

Compound	$\lambda_{\text{abs}}$ [nm]	$\lambda_{\text{f}}$ [nm]	$\Phi_{\text{f}}$	$E_{\text{s}}$ [eV]	$\epsilon$ [ $\text{M}^{-1}\text{cm}^{-1}$ ]	$\tau_{\text{s}}$ [ps]	$\tau_{\text{T}}$ [ $\mu\text{s}$ ]	$\Phi_{\text{ox}}^{\text{(DPBF)}}$	$\Phi_{\Delta}^{\text{(luminesc.)}}$
<b>5</b>	673	754	0.0065	1.65	48 000	$108 \pm 1$	-	0.00	0.00
<b>6</b>	789	838	0.0056	1.48	83 000	$100 \pm 1$	$21 \pm 2$	0.00	0.00
<b>7</b>	769	838	0.0076	1.48	55 000	$99 \pm 1$	$22 \pm 2$	$0.055 \pm 0.002$	0.00

$\lambda_{\text{abs}}$ : absorption band maximum in THF,  $\lambda_{\text{f}}$ : fluorescence band maximum in THF at RT,  $\Phi_{\text{f}}$ : fluorescence quantum yield measured in THF (indocyanine green was used as a reference compound with  $\Phi_{\text{f}} = 0.16$  in MeOH for **6** and **7**),  $E_{\text{s}}$ : energy of singlet excited state,  $\epsilon$ : molar absorption coefficient at  $\lambda_{\text{abs}}$  in THF,  $\tau_{\text{s}}$ : lifetime of excited singlet state in THF,  $\tau_{\text{T}}$ : lifetime of excited triplet in THF,  $\Phi_{\text{ox}}^{\text{(DPBF)}}$ : quantum yield of DPBF oxidation in THF,  $\Phi_{\Delta}^{\text{(luminesc.)}}$ : quantum yield of singlet oxygen in THF measured using the luminescence method.

At room temperature in THF solutions, the fluorescence maximum was observed at  $\lambda_f = 754$  nm (Stokes shift of 81 nm) for **5**, at  $\lambda_f = 838$  nm (Stokes shift of 49 nm) for **6** and at  $\lambda_f = 838$  nm (Stokes shift of 69 nm) for **7**. Compounds **5**, **6** and **7** can be deemed nearly non-fluorescent, because only negligible fluorescence was recorded with fluorescence quantum yields ( $\Phi_f$ ) below 1%. Based on the fluorescence spectra the following singlet excited state ( $S_1$ ) energies were calculated:  $E_s = 1.65$  eV for **5**,  $E_s = 1.48$  eV for **6** and **7**, respectively.

We believe, that the lack of torsional rigidity may induce the internal conversion in **5-7** leading to negligible emission. It has been described by several authors that rigidification of the aza-BODIPY structure leads to an increase of fluorescence quantum yield ( $\Phi_f$ ) [21]. Also, for the ADPM **5** additional phenomena may contribute to the lack of a noticeable fluorescence, namely, the possible tautomerization of the aza-dipyrromethene (migration of the proton between the adjacent pyrrole rings) that provides an efficient funnel for the non-radiative deactivation of the excited singlet state ( $S_1$ ) [72]. We also speculate that the intramolecular charge transfer (ICT) nature of the excited state in **5-7** exerted by the presence of strongly electron-donating *p*-(diphenylamino)phenyl substituents enhances the non-radiative decay and is responsible for the lack of strong emission in these compounds.

### 2.3. Time-resolved spectroscopy

We have investigated both the excited singlet ( $S_1$ ) and excited triplet ( $T_1$ ) state dynamics by recording femtosecond and nanosecond time-resolved transient absorption spectra, respectively. The transient absorption spectra, transient decays and singlet ( $\tau_s$ ) and triplet ( $\tau_T$ ) state lifetimes of **5-7** are presented in Figures 6 and 7 and summarized in Table 1.

Femtosecond flash photolysis allowed observation of excited singlet-state transient absorption spectra ( $S_1 \rightarrow S_n$ ) and dynamics ( $S_1 \rightarrow S_0$ ) in THF (Figure 6). The transient absorption spectra of **5-7** feature a positive  $S_1 \rightarrow S_n$  absorption band spanning from ca. 440 nm to ca. 600 nm, superimposed with ground state bleaching signal ( $S_1 \rightarrow S_0$ ). The decay of the transient  $S_1 \rightarrow S_n$  absorption and the recovery of the ground state absorption  $S_1 \rightarrow S_0$  were used to calculate singlet lifetimes ( $\tau_s$ ) of the investigated compounds **5-7**, with both methods giving similar values of  $\tau_s$ . Furthermore, for **5-7**, mono-exponential decays of the

transient absorption and recovery of the ground state absorption were observed. All compounds studied had very short-living excited singlet state ( $\tau_S$ ) in the picosecond range. ADPM **5** was found to have an excited singlet lifetime of ( $\tau_S$ ) 108 ps, aza-BODIPY **6** showed excited singlet lifetime of ( $\tau_S$ ) 100 ps while the brominated derivative **7** had nearly same excited singlet lifetime as its non-brominated congener **6**, viz.  $\tau_S = 99$  ps. These excited singlet lifetimes ( $\tau_S$ ) results were in very good agreement with the excited singlet lifetimes ( $\tau_S$ ) calculated from the fluorescence decays.

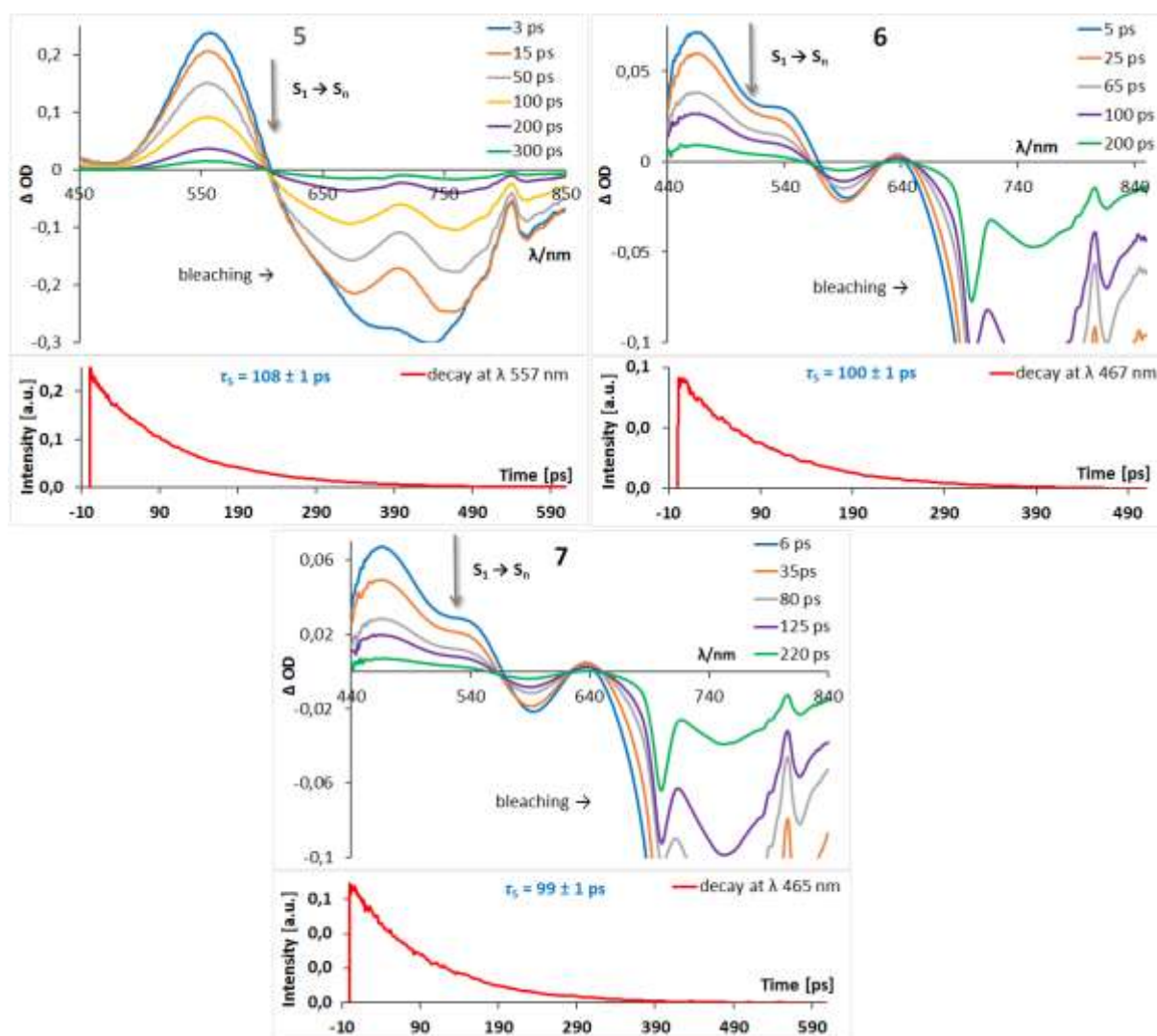


**Figure 6.** Femtosecond flash photolysis of **5**, **6** and **7** in THF at room temperature (laser energy 2  $\mu$ J, excitation wavelength  $\lambda_{ex}$  700 nm). Transient decays were monitored at  $\lambda$  557 nm for **5**,  $\lambda$  467 nm for **6** and  $\lambda$  465 nm for **7**, respectively.

In order to observe the excited triplet-state transient spectra ( $T_1 \rightarrow T_n$ ) and dynamics we changed the time domain of the measurements from femtosecond to nanosecond flash photolysis. Upon laser photolysis ( $\lambda_{\text{ex}}$  355 nm) of deaerated THF solution of ADPM **5** no observable transient absorption spectra were recorded. Introducing  $\text{BF}_2$  moiety into the ADPM **5** to form aza-BODIPY **6** and further bromination of **6** to mono-bromo derivative **7** produced two compounds with pronounced and observable triplet state. The nanosecond transient absorption spectra of **6** and **7** exhibit a broad positive  $T_1 \rightarrow T_n$  absorption band spanning from ca. 350 nm to ca. 550 nm, superimposed with the ground state bleaching signal. The mono-exponential decay of the  $T_1 \rightarrow T_n$  absorption was used to calculate the triplet lifetimes ( $\tau_T$ ) of both **6** and **7**. Both aza-BODIPYs had very similar triplet lifetimes:  $\tau_T$  of  $21 \pm 2 \mu\text{s}$  was found for **6** and  $\tau_T$  equaled to  $22 \pm 2 \mu\text{s}$  for **7**. After saturating the THF solutions of **6** and **7** with air for 1 minute the observed kinetics shortened substantially to approximately  $\tau_T = 1.5 \mu\text{s}$  for both aza-BODIPYs. This observation provides irrefutable evidence that the observed transient absorptions originated from the excited triplet-state ( $T_1 \rightarrow T_n$ ).

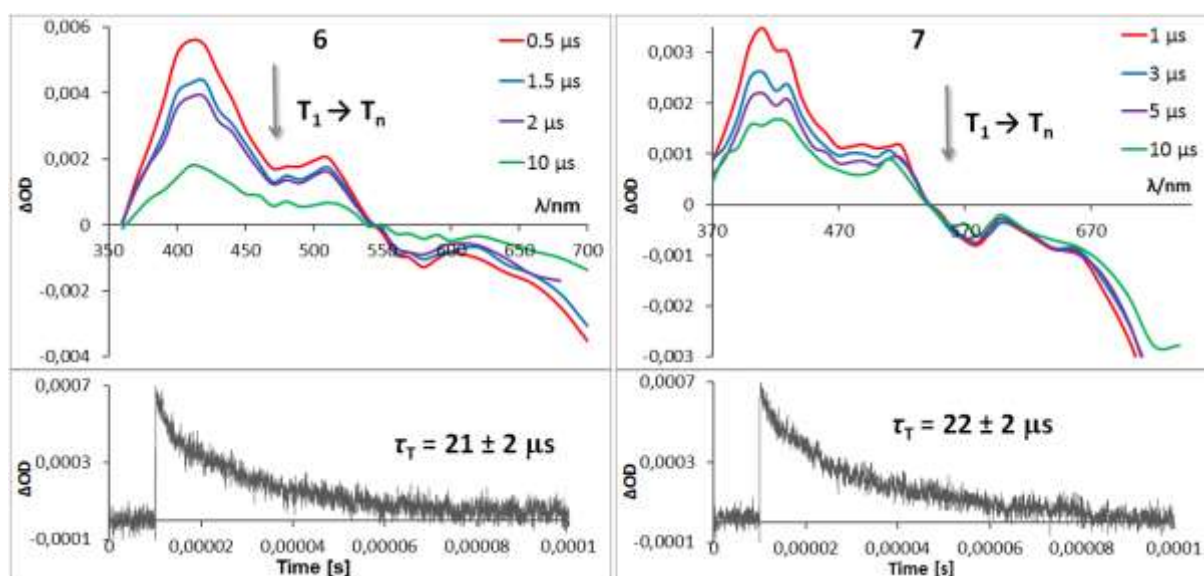


**Figure 7.** Nanosecond transient absorption spectra of aza-BODIPY **6** and **7** measured in THF at room temperature with excitation wavelength  $\lambda_{\text{ex}} = 355 \text{ nm}$  and laser energy 3.0 mJ/pulse. Transient decays (at the bottom) monitored at  $\lambda = 410 \text{ nm}$  with laser energy 0.5 mJ/pulse (to avoid triplet-triplet annihilation).

## 2.4. Photosensitization

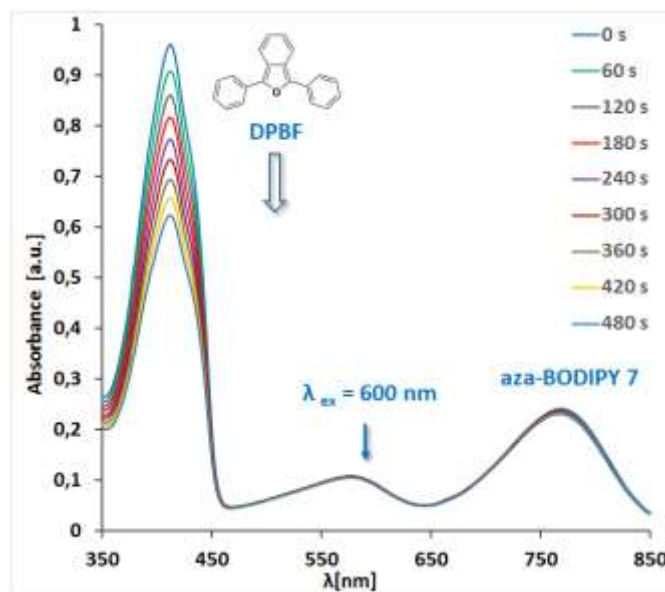


**Figure 8.** Photosensitized degradation of 1,3-diphenylisobenzofuran (DPBF) initiated by aza-BODIPY **7** in THF.

The ability of halogenated aza-BODIPY **7** to sensitize the formation of singlet oxygen ( $^1\text{O}_2$ ) and/or other reactive forms of oxygen (ROS) was considered and quantitatively assessed as singlet oxygen quantum yield ( $\Phi_\Delta$ ) and quantum yield of DPBF oxidation ( $\Phi_{\text{ox}}^{\text{(DPBF)}}$ ), respectively. In order to determine the value of  $\Phi_{\text{ox}}^{\text{(DPBF)}}$  and  $\Phi_\Delta$  and of **7** we resorted to two methods, viz. the indirect method based on a chemical quencher and the direct method based on the observation of singlet oxygen phosphorescence [74]. In the first method, the progress of the reaction between the reactive oxygen species (ROS) formed upon photosensitization with the compound studied and the well-known chemical quencher (viz. 1,3-diphenylisobenzofuran, DPBF) was followed by the observation of the decay of the absorption band of DPBF at  $\lambda$  417 nm. The second method relied on the observation of the intensity of the luminescence of singlet oxygen ( $^1\text{O}_2$ ) at  $\lambda$  1270 nm formed upon photosensitization with the compound studied and the standard compound with known value of singlet oxygen quantum yield ( $\Phi_\Delta$ ). The luminescence method allows exclusive detection of singlet oxygen ( $^1\text{O}_2$ ), while in the method utilizing a chemical quencher, the DPBF employed reacts indistinguishably with both singlet oxygen ( $^1\text{O}_2$ ) and the radicals

formed (viz.  $\text{OH}^\bullet$ ,  $\text{HO}_2^\bullet$ ,  $\text{O}_2^{\bullet-}$ ,  $\text{R}^\bullet$ ,  $\text{R}^{\bullet+}$ ,  $\text{ROO}^\bullet$ ,  $\text{RO}^\bullet$ ) [75]. Comparison of the values obtained by both methods gives an insight into the relative contribution of Type II (singlet oxygen formation), Type I (hydrogen atom abstraction) and Type III (electron transfer) mechanisms of the photo-oxygenation initiated by the photosensitizers tested [76]. Interestingly, when the oxygen saturated THF solution of aza-BODIPY **7** was excited at its  $\lambda_{\text{abs}}$  a gradual depletion of the absorption band of the chemical quencher was observed pointing to the formation of singlet oxygen and/or other ROS (Figure 8). A quantum yield of DPBF oxidation  $\Phi_{\text{ox}}^{\text{(DPBF)}} = 0.055 \pm 0.002$  was found for mono-brominated aza-BODIPY **7**. Importantly, no luminescence originating from singlet oxygen ( $^1\text{O}_2$ ) was discernible at  $\lambda$  1270 nm upon excitation of the oxygen saturated THF solution of **7**. A comparison of these two experiments clearly indicates that the photo-oxygenation of DPBF with aza-BODIPY **7** as the photosensitizer does not occur via Type II mechanism but it involves either hydrogen abstraction (Type I) and/or electron transfer (Type III) mechanism.

## 2.5. Electrochemistry and HOMO/LUMO energy levels

**Table 2.** The frontier energy levels [eV] and redox potentials [V] vs.  $\text{Fc}/\text{Fc}^+$  for **5**, **6** and **7** obtained from differential pulse voltammetry (DPV). Glassy carbon electrode was used as a working electrode.

Data collected in 1,2-dichlorobenzene with 0.1 M tetrabutylammonium tetrafluoroborate as supporting electrolyte.

Compound	$E_{\text{ox}}^1$ [V]	$E_{\text{ox}}^2$ [V]	$E_{\text{red}}^1$ [V]	$E_{\text{red}}^2$ [V]	$E_{\text{LUMO}}^a$ [eV]	$E_{\text{HOMO}}^b$ [eV]	$E_g$ (electro) <sup>c</sup> [eV]
<b>5</b>	+ 0.06	+ 0.23	- 1.54	- 2.13	- 3.56	- 5.16	1.60
<b>6</b>	+ 0.18	+ 0.43	- 1.10	- 1.91	- 4.00	- 5.28	1.28
<b>7</b>	+ 0.31	+ 0.53	- 1.04	- 1.76	- 4.06	- 5.41	1.35

<sup>a</sup>  $E_{\text{LUMO}} = - (E_{[\text{first reduction vs. Fc/Fc}^+]} + 5.1)$  [eV], <sup>b</sup>  $E_{\text{HOMO}} = - (E_{[\text{first oxidation vs. Fc/Fc}^+]} + 5.1)$  [eV], <sup>c</sup>  $E(\text{electro}) = \text{electrochemical gap}$ .

Differential pulse voltammetry (DPV) and cyclic voltammetry (CV) measurements were performed in an effort to estimate the electrochemical properties of compounds **5** to **7** ( $E_{\text{ox}}^1$

and  $E_{\text{red}}^1$ ), to estimate the HOMO/LUMO energy levels and to comprehend the impact of both *para*-diphenylamino groups ( $\text{Ph}_2\text{N-}$ ) and halogen substituents on the electrochemical properties of the compounds studied. The results were summarized in Table 2 and presented in Figure 9. In order to elucidate the nature of the redox processes observed and to shed more light on the relative stabilities of the reduced and oxidized species formed, a thin-layer spectroelectrochemistry was performed (Figure 10).

Both the DPV and CV measurements indicated the presence of two oxidation processes within the potential range applied ( $E_{\text{ox}}^1$ ,  $E_{\text{ox}}^2$ ) with the first oxidation potential ( $E_{\text{ox}}^1$ ) occurring at a relatively low potential - indicating an ease to undergo oxidation process (low ionization potential). This observation is in line with the electron-donating nature of the *para*-diphenylamino groups ( $\text{Ph}_2\text{N-}$ ). ADPM **5** was the easiest of all the compounds studied to oxidize with the first oxidation potential ( $E_{\text{ox}}^1$ ) found at a value of + 0.06 V vs.  $\text{Fc}/\text{Fc}^+$ . Controlled potential electrolysis of AcCN solution of **5** at + 0.4 V vs.  $\text{Ag}/\text{Ag}^+$ , where  $E_{\text{ox}}^1$  occurs, resulted in the emergence of redshifted band at  $\lambda$  970 nm at the expense of the band at  $\lambda$  690 nm. Such spectral changes are associated with the formation of a cation radical ( $\text{ADPM}^{\bullet+}$ ). Switching the potential to a more negative allowed the recovery of the initial absorption spectrum of ADPM **5**, meaning that the first electrochemical oxidation was a chemically reversible process. In turn, controlled potential electrolysis of **5** at a potential of - 1.1 V vs.  $\text{Ag}/\text{Ag}^+$ , where  $E_{\text{red}}^1$  occurs, resulted in irreversible degradation of the reduced form of **5** (Figure S1). Incorporation of difluoroboron moiety ( $\text{BF}_2$ ) into the binding pocket of the ligand **5** had the effect of shifting the first oxidation potential ( $E_{\text{ox}}^1$ ) to a more positive value, viz. + 0.18 V vs.  $\text{Fc}/\text{Fc}^+$  - an observation in accordance with the electron-deficient nature of the  $\text{BF}_2$  moiety. Controlled potential electrolysis of AcCN solution of **6** at + 0.43 V vs.  $\text{Ag}/\text{Ag}^+$ , viz. at  $E_{\text{ox}}^1$ , resulted in the emergence of NIR band at  $\lambda$  1035 nm at the expense of the bands at  $\lambda$  805 nm and  $\lambda$  580 nm (Figure 10). The observed spectral changes were ascribed to the formation of the cation radical (aza-BODIPY $^{\bullet+}$ ). Switching the potential to a more negative allowed recovery of the initial absorption spectrum of **6**, meaning that the first electrochemical oxidation was a chemically reversible process within the timeframe of the experiment. Controlled potential electrolysis of AcCN solution of **6** at the potential where first reduction occurs (viz. - 1.0 V vs.  $\text{Ag}/\text{Ag}^+$ ) resulted in anion radical formation, viz. aza-BODIPY $^{\bullet-}$ , marked by evolution of two absorption bands at  $\lambda$  870 nm and  $\lambda$  460 nm (a

reversible process upon applying a more positive potential). Adding the bromine atom to one of the pyrrole rings at 2 position (Scheme 1) further shifted the first oxidation potential ( $E_{\text{ox}}^1$ ) to a more positive value for compound **7**, viz. + 0.31 V vs. Fc/Fc<sup>+</sup>.

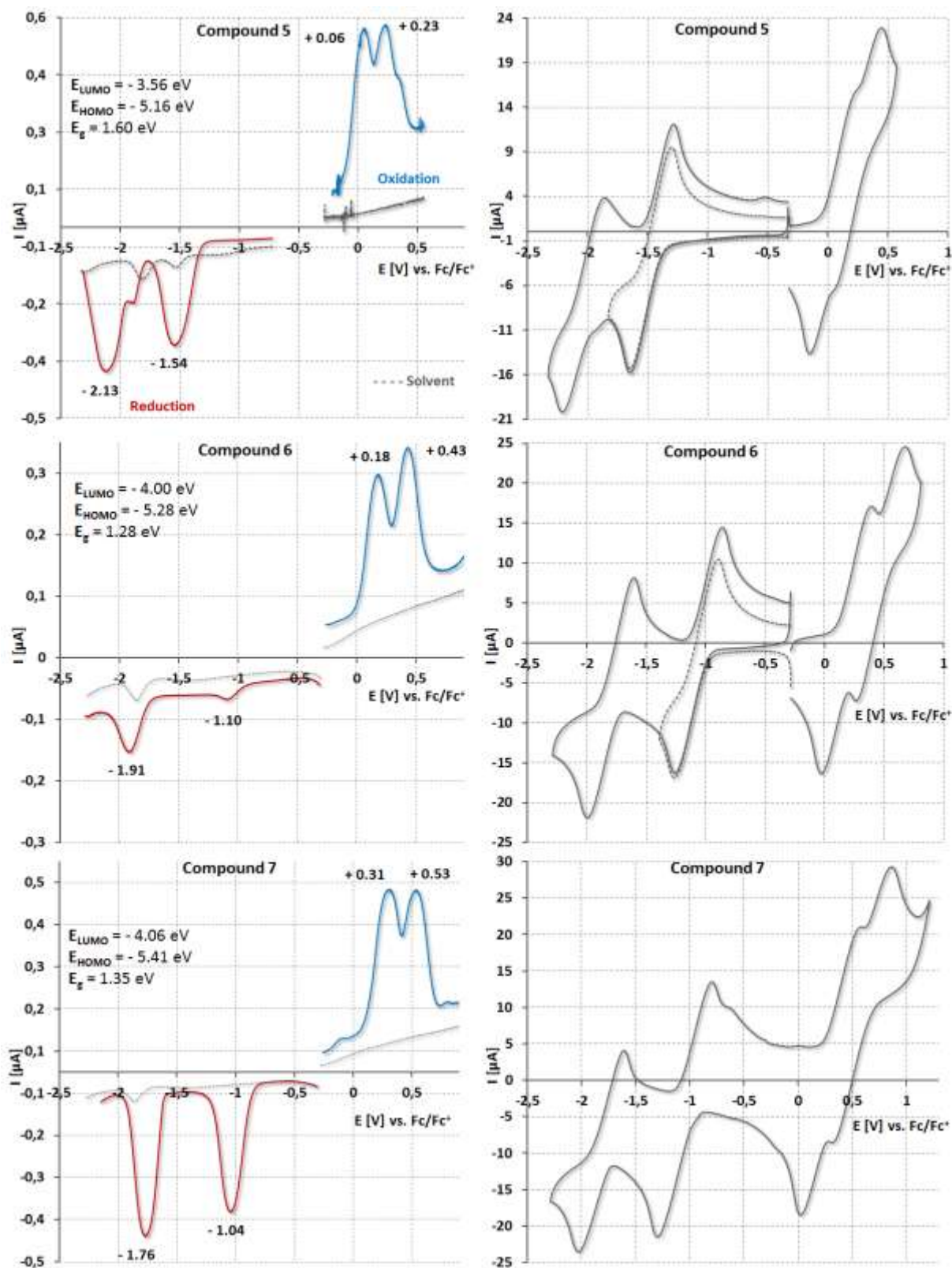


**Figure 9.** Differential pulse voltammetry and cyclic voltammetry of **5**, **6** and **7**. Data were collected on glassy carbon working electrode in *o*-dichlorobenzene with 0.1 M *n*Bu<sub>4</sub>NBF<sub>4</sub> as the supporting electrolyte at a scan rate of 100 mVs<sup>-1</sup> (cyclic voltammetry). Redox potentials are reported in reference to the ferrocene/ferrocenium redox couple.

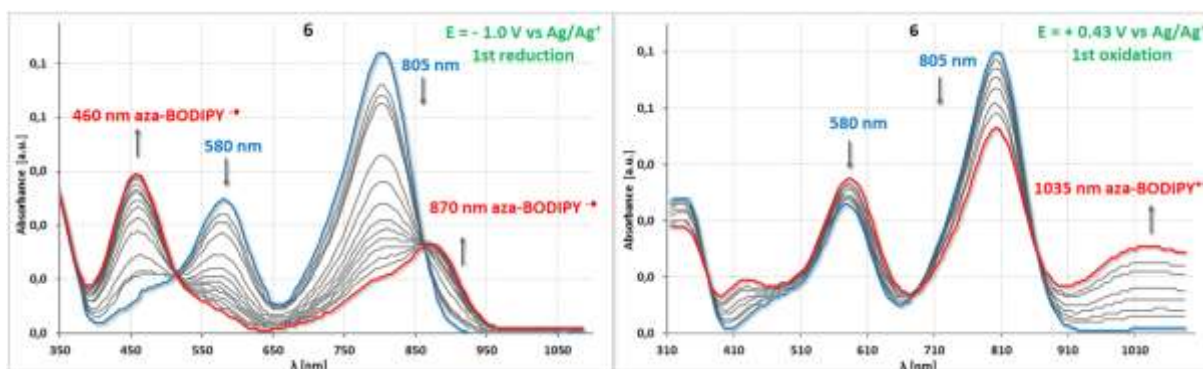


**Figure 10.** UV-Vis spectra of aza-BODIPY **6** collected during electrolysis at two different potentials, viz. - 1.0 V and + 0.43 V vs Ag/Ag<sup>+</sup>. Data collected in 1,2-dichlorobenzene with 0.1 M tetrabutylammonium tetrafluoroborate as supporting electrolyte with Pt working electrode.

Two reduction processes were discernible for compounds **5-7**. Both oxidation and reduction processes observed for **5-7** could be deemed as electrochemically irreversible process in terms of the electron transfer kinetics ( $\Delta E = E_{p,a} - E_{p,c}$ , ca. 340 mV to 550 mV). ADPM **5** was the hardest to reduce out of all compounds studied with the first reduction potential ( $E_{red}^1$ ) observed at - 1.54 V vs. Fc/Fc<sup>+</sup>. Given the electron-deficient nature of the BF<sub>2</sub> moiety, incorporation of BF<sub>2</sub> into the ligand **5** to form aza-BODIPY **6**, significantly shifted the first reduction potential ( $E_{red}^1$ ) to - 1.10 V vs. Fc/Fc<sup>+</sup>. Adding bromine atom to one of the pyrrole rings at 2 position had virtually no impact on the first reduction potential ( $E_{red}^1$ ) of aza-BODIPY **7**, viz.  $E_{red}^1 = - 1.04$  V vs. Fc/Fc<sup>+</sup>.

The values of the first reduction ( $E_{red}^1$ ) and oxidation ( $E_{ox}^1$ ) potentials were used to calculate the energy levels of the LUMO ( $E_{LUMO}$ ) and HOMO ( $E_{HOMO}$ ), assuming that the formal potential of the Fc/Fc<sup>+</sup> redox couple equals - 5.1 eV in the Fermi scale (Table 2) [77-78]. The following equations were used:  $E_{LUMO} = - (E_{[first\ reduction\ vs.\ Fc/Fc^+]} + 5.1)$  [eV] and  $E_{HOMO} = - (E_{[first\ oxidation\ vs.\ Fc/Fc^+]} + 5.1)$  [eV]. Estimation of the  $E_{LUMO}$  gave the value of - 3.56 eV for **5**, - 4.00 eV for **6** and - 4.06 eV for **7**, respectively. The  $E_{HOMO}$  was found to be located at - 5.16 eV for **5**, - 5.28 eV for **6** and - 5.41 eV for **7**, respectively. Adding BF<sub>2</sub> moiety to the binding pocket of the ADPM **5** had the effect of lowering the energy of the LUMO( $E_{LUMO}$ ) and only slightly affected the energy of the HOMO ( $E_{HOMO}$ ). Moreover, bromination of the pyrrole ring at 2

position (compounds **7**) had no impact on  $E_{\text{LUMO}}$  and only slightly lowered the  $E_{\text{HOMO}}$ . The electrochemical energy gaps ( $E_g$ ) calculated as the difference between the first oxidation and first reduction potentials equaled 1.60 eV for the ADPM **5**, 1.28 eV for aza-BODIPY **6** and 1.35 eV for the mono-brominated derivative **7**.

## 2.6. Photostability and thermal stability

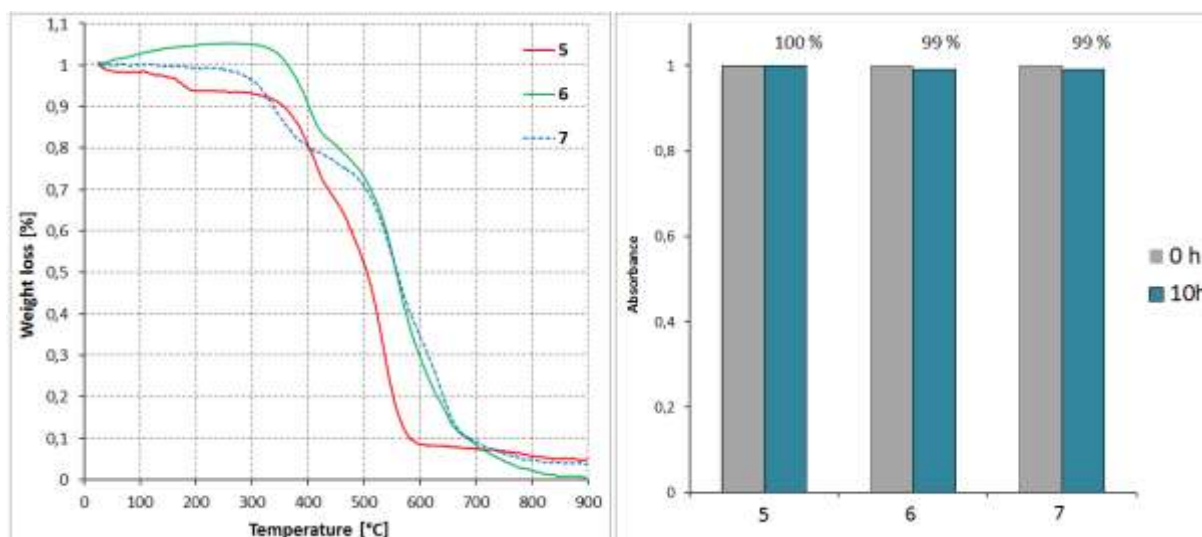


**Figure 11.** TGA profiles (left panel, heating rate  $10^{\circ}\text{Cmin}^{-1}$ , aerobic conditions) and UV/Vis monitored photostability of compounds **5**, **6** and **7** in THF solutions exposed to the irradiation at  $\lambda > 473$  (right panel) and  $I = 1000 \pm 50 \text{ W/m}^2$ .

The stability of compounds **5-7** was tested in terms of both thermal stability and photostability. The thermogravimetric profiles obtained for **5-7** under aerobic conditions indicated good thermal stability up to approximately 300 °C (Figure 11). The THF solutions of **5-7** were exposed to the bright light of a xenon lamp ( $1000 \pm 50 \text{ W/m}^2$ ) separated from the samples with a 473 nm cut-off filter under aerobic conditions (Figure 11). UV/Vis spectra were taken over time in an effort to assess the relative photostability of the ADPM **5** and aza-BODIPYs **6** and **7** studied. After 10 h of irradiation no loss of the initial intensity of the

absorption band was observed for compound **5** and merely 1% loss of the initial intensity of the absorption band was detected for compounds **6** and **7**, respectively. These findings point to an outstanding photostability of **5-7** under the experimental conditions applied. This finding is of prime importance in view of the fact that materials suitable for photocatalysis and optoelectronic applications should be characterized by high durability under photoirradiation.

### 3. Discussion

Synthesis of organic dyes capable of light absorption from the NIR part of the spectrum with concomitant ability to sensitize formation of singlet oxygen ( $^1\text{O}_2$ ) and/or other reactive forms of oxygen (ROS) is a promising but challenging research field with only scarce literature reports on such photosensitizers. One of the most frequently employed strategies to induce NIR absorption in a given chromophore system relies on modifying the structure with strongly electron-donating groups (amino groups in particular, see Introduction). Presence of such groups lowers the energy of the singlet excited state ( $E_s$ ) and shifts the absorption band ( $\lambda_{\text{abs}}$ ) beyond the visible part of the spectrum. However, presence of strongly electron-donating amino groups (either  $\text{Me}_2\text{N-}$  or  $\text{Ph}_2\text{N-}$ ) may also result in some unfavorable phenomena that diminish ability of such molecule to efficiently populate triplet excited state ( $E_T$ ) and generate ROS. In one of our recent papers we reported synthesis and properties of NIR absorbing aza-BODIPY substituted with *p*-(dimethylamino)phenyl groups – a structure that closely resembles aza-BODIPY reported herein [71]. In the same paper we reported properties of several poly-halogenated derivatives of *p*-( $\text{Me}_2\text{N}$ )Ph- substituted aza-BODIPY. We observed a pronounced intramolecular charge transfer (ICT) exerted by the presence of strongly electron-donating *p*-( $\text{Me}_2\text{N}$ )Ph- groups resulting in lack of highly populated triplet excited state ( $T_1$ ), relatively low lifetime of triplet excited state ( $\tau_T = 6 \mu\text{s}$ ) and inability of these aza-BODIPYs to sensitize formation of  $^1\text{O}_2$  and other ROS ( $\Phi_\Delta = 0$ ). Herein, we demonstrated that by replacing the dimethylamino groups ( $\text{Me}_2\text{N-}$ ) with a diphenylamino ( $\text{Ph}_2\text{N-}$ ) groups we managed to slightly diminish the extent of ICT, increase the excited triplet lifetime to  $\tau_T = 22 \mu\text{s}$  and induce photosensitizing properties in compound **7** ( $\Phi_{\text{ox}}^{(\text{DPBF})} = 0.055$ ). However, the value of  $\Phi_{\text{ox}}^{(\text{DPBF})}$  that we observed for *p*-(diphenylamino)phenyl

substituted aza-BODIPY reported herein is still too low for the dye to be used as a PDT photosensitizer or photocatalyst. A work is in progress in our laboratory to improve the photosensitizing properties of *p*-(diphenylamino)phenyl substituted aza-BODIPY while maintaining its ability to absorb light from the NIR part of the spectrum.

Also, via the electrochemical measurements we demonstrated that these compounds can be used as efficient electron donors with very low first oxidation potential ( $E_{ox}^1$ ). The *p*-(diphenylamino)phenyl substituents at 3,5 positions can act as an “electron reservoir” with the electron delocalization of the free electron pair of the Ph<sub>2</sub>N- group being the driving force for the efficient electron donation. Research and development dedicated to organic light-emitting diodes (OLEDs), organic field-effect transistors (OFETs) and dyes sensitized solar cells (DSSC) have been the subject of considerable attention in recent decades. Devices like organic electronics and optoelectronics require either electron-donating (p-type) or electron-accepting (n-type) materials. Given the very strong electron-donating character of the *p*-(Ph<sub>2</sub>N)Ph- substituted aza-BODIPY/ADPM described in this paper combined with high thermal stability, remarkable photostability, high molar absorption coefficient ( $\epsilon$ ) and low ionization potential, we postulate that these compounds maybe of great interest as photoactive/electroactive components of various organic electronics or optoelectronics. In Figure 12 we compared a set of aza-BODIPYs and aza-dipyrromethenes with both electron-donating and electron-accepting groups prepared and reported by our research group [69,71,72,79,80].

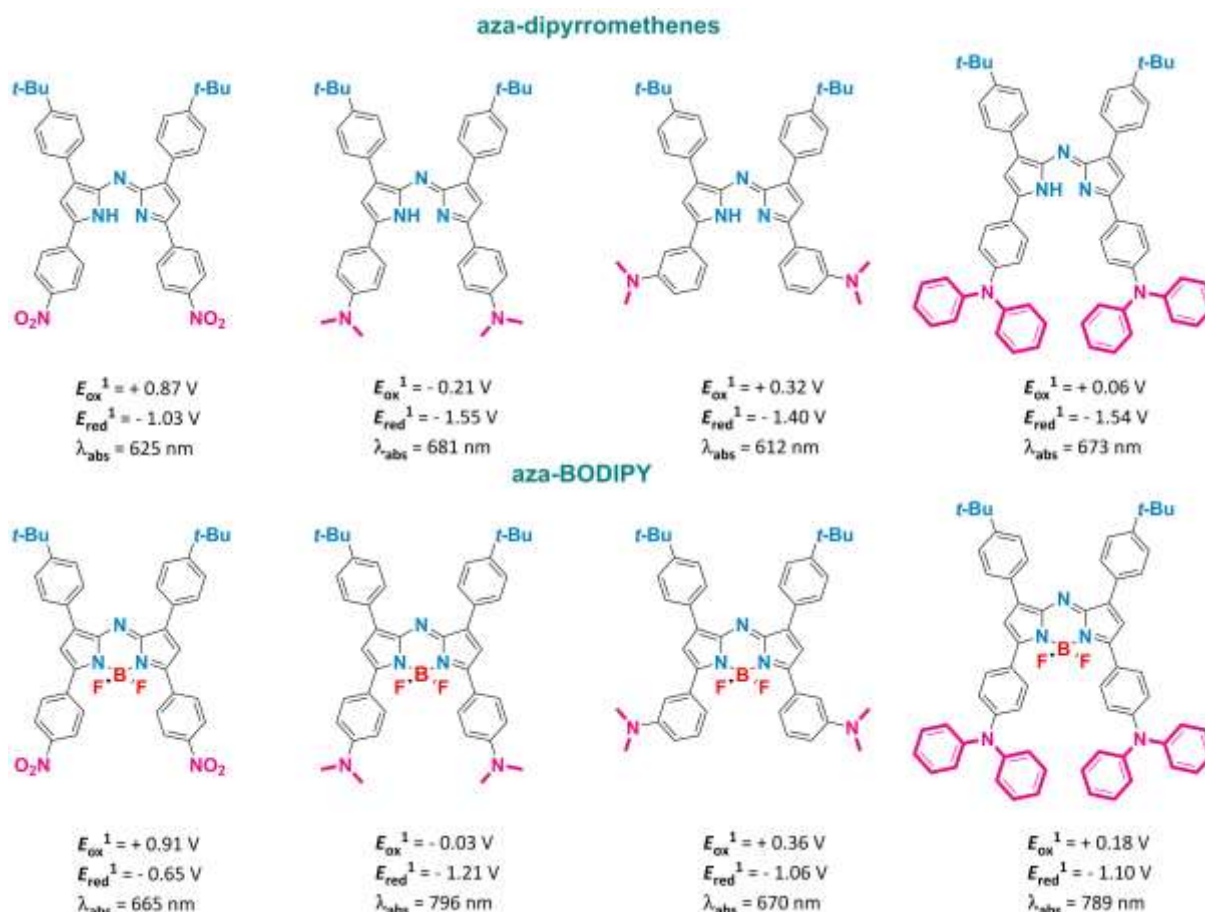


**Figure 12.** A comparison of optical ( $\lambda_{\text{abs}}$ , in THF) and electrochemical ( $E_{\text{ox}}^1$ ,  $E_{\text{red}}^1$  in 1,2-dichlorobenzene or THF) properties of aza-dipyrrromethenes and aza-BODIPYs bearing either electron-withdrawing or electron-donating substituents at 5,5' positions (aza-dipyrrromethene) or 3,5 positions (aza-BODIPY) prepared in our laboratory [69,71,72,79,80].

## 4. Experimental

### 4.1. Materials and methods

NMR spectra were recorded on Bruker Avance III HD 400 MHz in deuterated solvents. Electrospray mass spectrometer microTOF II (Bruker Daltonics, Bremen/Germany) with a resolution of > 16 500 FWHM and a mass accuracy of < 2 ppm was used to obtain the high-resolution mass spectra. FT-ATR-IR spectra were recorded using a Nicolet iS10 spectrometer. UV-Vis absorption spectra at RT were measured using a Hewlett-Packard 8452A diode-array spectrophotometer equipped with a HP 89090A Peltier temperature control accessory or HITACHI U-2910. Fluorescence spectra were collected using Cary Eclipse Agilent

spectrophotometer. For the elemental micro analysis, the CHNS Vario Micro Cube analyzer combined with the electronic microbalance was used. Compounds were analysed using a Thermo-gravimetric analyzer Mettler Toledo TGA/SDTA 851e and the analysis was carried out using samples of approximately 3-5 mg in weight and a heating rate of 10 °C min<sup>-1</sup> under air. Reaction progress was controlled using TLC on silica gel (Supelco). 1,2-Dichlorobenzene was dried with CaH<sub>2</sub> and freshly distilled prior to use. Triphenylamine (**1**) was purchased from TCI Europe and used as supplied.

## 4.2. Synthesis

**1-(4-(diphenylamino)phenyl)ethan-1-one (2)**: The described synthesis of **2** is a modification of the procedure reported elsewhere [73]. Acetyl chloride (6.4 g, 5.8 ml, 81.53 mmol) was added dropwise via syringe to a slurry of triphenylamine (**1**; 20 g, 81.53 mmol) and ZnCl<sub>2</sub> (11.11 g, 81.53 mmol) in dry dichloromethane (80 ml) at 0 °C. When the addition of acetyl chloride was completed, the ice bath was removed and the reaction mixture was kept under refluxed for 24 h. The reaction mixture was poured over crushed ice and a mixture of concentrated hydrochloric acid (20 ml) and water (60 ml) was added. After 0.5 h of stirring the acidify mixture was neutralized with a solution of Na<sub>2</sub>CO<sub>3</sub>. The crude product was extracted with a dichloromethane and the organic layer was washed with water (3 x 100 ml). The crude product was pre-adsorbed onto a silica gel and twice chromatographed on a column filled with a silica gel (5 cm x 18 cm). A mixture of toluene and hexane (1:1) was used as an eluent. The purity of fractions collected was controlled with a TLC (silica gel; acetone/hexane, 2:8). Yield: 10.56 g (45 %), white solid. **<sup>1</sup>H NMR** (600 MHz, CDCl<sub>3</sub>) δ: 7.80 (d, *J* = 8.9 Hz, 2H), 7.32 (dd, *J* = 8.4, 7.4 Hz, 4H), 7.17 – 7.12 (m, 6H), 6.99 (d, *J* = 8.9 Hz, 2H), 2.53 (s, 3H). **<sup>13</sup>C NMR** (151 MHz, CDCl<sub>3</sub>) δ: 196.6, 152.3, 146.6, 130.0, 129.9, 129.8, 126.1, 124.8, 119.8, 26.4. **HR-ESI-MS**: calcd for C<sub>20</sub>H<sub>17</sub>NONa [M+Na<sup>+</sup>]<sup>+</sup> 310.1202. Found: 310.1202. **FT-ATR-IR**: ν (cm<sup>-1</sup>) = 3324, 3036, 3005, 1669, 1579, 1486, 1416, 1356, 1329, 1262, 1170, 1114, 1073, 951, 842, 819, 695. **Anal. Calcd** for C<sub>20</sub>H<sub>17</sub>NO: C, 83.59 %, H, 5.97 %, N, 4.88 %. Found: C, 83.39 %, H, 6.00 %, N, 4.77 %.

**3-(4-(tert-butyl)phenyl)-1-(4-(diphenylamino)phenyl)prop-2-en-1-one (3)**: NaOH (4.5 g, 11.25 mmol) was dissolved in EtOH (50 ml). This solution was slowly added to a vigorously stirred mixture of 4-*tert*-butylbenzaldehyde (6.1 g, 37.6 mmol) and 1-(4-

(diphenylamino)phenyl)ethan-1-one (**2**; 10.563 g, 36.76 mmol) in ethanol (550 ml). The temperature of the reaction mixture was kept at 0 °C during addition of the base. After 0.5 h the ice bath was removed and the reaction mixture was allowed to reach the room temperature. The reaction mixture was stirred at room temperature for 24h. The formation of a yellow, crystalline solid was observed. Water was added dropwise to the reaction mixture under vigorous stirring and the precipitate formed was filtered and washed with a copious amount of water, and then twice with a mixture of acetonitrile/water (45 ml/55 ml). The crude product was purified by column chromatography (silica gel; toluene/hexane, 1:1). Pure fraction were collected. Impure fractions were combined together and re-purified by a column chromatography (silica gel; toluene/hexane, 1:1). Yield: 10.91 g (69 %), a yellow solid. <sup>1</sup>H NMR (600 MHz, CDCl<sub>3</sub>) δ: 7.92 (d, *J* = 8.9 Hz, 2H), 7.81 (d, *J* = 15.6 Hz, 1H), 7.58 (d, *J* = 8.3 Hz, 2H), 7.51 (d, *J* = 15.6 Hz, 1H), 7.44 (d, *J* = 8.4 Hz, 2H), 7.33 (dd, *J* = 8.4, 7.5 Hz, 4H), 7.18 (dd, *J* = 8.5, 1.0 Hz, 4H), 7.15 (t, *J* = 7.4 Hz, 2H), 7.05 (d, *J* = 8.8 Hz, 2H), 1.35 (s, 9H). <sup>13</sup>C NMR (75 MHz, CDCl<sub>3</sub>) δ: 188.5, 154.0, 152.1, 146.7, 143.7, 132.6, 130.9, 130.2, 129.7, 128.3, 126.1, 126.0, 124.7, 121.2, 120.0, 35.0, 31.3. **HR-ESI-MS**: calcd for C<sub>31</sub>H<sub>29</sub>NO [M]<sup>+</sup>: 454.2141. Found: 454.2141. **FT-ATR-IR**: ν (cm<sup>-1</sup>) = 3035, 2959, 2865, 1656, 1633, 1581, 1486, 1418, 1326, 1273, 1221, 1170, 1112, 1074, 1026, 973, 817, 751, 696. **Anal.** Calcd for C<sub>31</sub>H<sub>29</sub>NO: C, 86.27 %, H, 6.78 %, N, 3.25 %. Found: C, 85.54 %, H, 6.77 %, N, 3.12 %.

**3-(4-(tert-butyl)phenyl)-1-(4-(diphenylamino)phenyl)-4-nitrobutan-1-one (4)**: Compound **3** (12.686 g, 29.41 mmol), nitromethane (2.153 g, 35.29 mmol), K<sub>2</sub>CO<sub>3</sub> (1 g, 7.23 mmol) and methanol (350 ml) were combined in a flask. The reaction mixture was kept under reflux for 17 hours. The solvent was removed on a rotary evaporator. The crude product was pre-adsorbed onto a silica gel and purified by column chromatography (SiO<sub>2</sub>; toluene/hexane 2:1). The purity of the fractions was controlled with a TLC (silica gel; toluene/hexane, 2:1). The chromatography performed allowed only partial purification. 15.135 g of impure product in the form of oil was collected. Neither chromatography nor crystallization allowed isolation of pure product. As all attempts to purify the product **5** failed it was decided to use the impure product for the next reaction step. However, in order to spectroscopically confirm formation of **4** a small sample of the impure product (123 mg) was purified by a preparative TLC (MERCK, PLC Silica gel 60 F<sub>245</sub>, 2 mm, 20mx20cm) with a mixture of acetone and hexane (1:9 v/v) as an eluent. The preparative TLC plate was developed four times

before collecting the pure product. Yield: 93 mg, 79 %. **<sup>1</sup>H NMR** (600 MHz, CDCl<sub>3</sub>) δ: 7.75 (d, *J* = 8.9 Hz, 2H), 7.35 – 7.30 (m, 6H), 7.20 (d, *J* = 8.3 Hz, 2H), 7.17 – 7.12 (m, 6H), 6.95 (d, *J* = 8.9 Hz, 2H), 4.82 (dd, *J* = 12.5, 6.5 Hz, 1H), 4.67 (dd, *J* = 12.5, 8.2 Hz, 1H), 4.22 – 4.13 (m, 1H), 3.37 (dd, *J* = 17.3, 6.0 Hz, 1H), 3.30 (dd, *J* = 17.3, 7.9 Hz, 1H), 1.29 (s, 9H). **<sup>13</sup>C NMR** (75 MHz, CDCl<sub>3</sub>) δ: due to the overlap of many resonance signals we do not report the <sup>13</sup>C NMR spectrum for this compound. **HR-ESI-MS**: calcd for C<sub>32</sub>H<sub>32</sub>N<sub>2</sub>O<sub>3</sub>Na [M+Na<sup>+</sup>]<sup>+</sup>: 515.2305. Found: 515.2305. **FT-ATR-IR**: ν (cm<sup>-1</sup>) = 3059, 2960, 2867, 1668, 1583, 1549, 1488, 1422, 1374, 1323, 1268, 1230, 1172, 1114, 1074, 978, 905, 829, 755, 729, 695.

**ADPM (5)**: Compound **4** (4.98 g, given that the crude product contains 79% of the compound **4** it accounts for 7.99 mmol of **4**), ammonium acetate (30 g, 389.2 mmol) and n-butanol (20 ml) were combined in a flask and heated under reflux (117 °C) for 1.5 h after which time another portion of ammonium acetate was added to the reaction mixture and the stirring was continued for an additional 1.5 h (total reaction time: 3 h). The solution was cooled and the precipitate formed was filtered and washed with methanol. The crude product was dissolved in acetone (40 ml) and water was added dropwise to the stirred acetone solution until all compound precipitated. The precipitate formed was filtered and washed with water and methanol. The crude product was pre-adsorbed onto a few grams of silica gel and passed through a glass column (30 cm) filled with silica gel (flash chromatography). A mixture of toluene and hexane (1:1, v/v) was used as an eluent. An intense blue fraction was collected and the solvent was removed. The flash chromatography was repeated two more times in the same manner. The partially purified product was dissolved in DCM (50 ml) and methanol was added dropwise (50 ml) to the solution. The solution was left overnight to form crystals of pure product (dark, shiny needles). The crystals formed were filtered and thoroughly washed with methanol. Yield: 2.253 g (63%). **<sup>1</sup>H NMR** analysis indicated that compound **6** co-crystallized with DCM in a 1:1 ratio.

**<sup>1</sup>H NMR** (600 MHz, CDCl<sub>3</sub>) δ: 8.00 (d, *J* = 8.4 Hz, 4H), 7.77 (d, *J* = 8.7 Hz, 4H), 7.44 (d, *J* = 8.4 Hz, 4H), 7.30 (m, 8H), 7.16 (d, *J* = 7.6 Hz, 8H), 7.12 (d, *J* = 8.7 Hz, 4H), 7.10 (t, *J* = 7.4 Hz, 4H), 1.39 (s, 18H), the signal of the pyrrole rings overlaps with the triplet at 7.10 ppm (2H). **<sup>13</sup>C NMR** (75 MHz, CDCl<sub>3</sub>) δ: 154.0, 150.9, 149.7, 149.5, 147.2, 142.1, 131.4, 129.6, 129.1, 127.6, 125.7, 125.4, 125.2, 124.1, 122.6, 114.0, 34.8, 31.5. **UV-Vis** (THF) λ nm (ε [M<sup>-1</sup>cm<sup>-1</sup>]): 673 (48 000). **HR-ESI-MS**: calcd for C<sub>64</sub>H<sub>57</sub>N<sub>5</sub> [M]<sup>+</sup>: 895.4608. Found: 895.4607. **FT-ATR-IR**: ν (cm<sup>-1</sup>) =

3035, 2956, 2862, 1581, 1545, 1486, 1456, 1406, 1330, 1313, 1264, 1167, 1146, 1105, 1022, 964, 902, 839, 801, 750, 694. **Anal.** Calcd for  $C_{65}H_{59}N_5Cl_2$  (this compound crystallizes as 1:1 complex with DCM) : C, 79.56 %, H, 6.07 %, N, 7.14 %. Found: C, 80.90 %, H, 6.14 %, N, 7.24 %.

**Aza-BODIPY (6):** Compound **5** (0.2 g, 0.223 mmol) was dissolved in freshly distilled and dried dichloromethane (20 ml). The solution was heated and kept under reflux in an inert gas atmosphere. Dry diisopropylamine (0.144 g, 0.2 ml, 1.43 mmol) was injected to the reaction mixture followed by 15 minutes of stirring.  $BF_3 \cdot OEt_2$  was added to the reaction mixture (0.34 g, 2.4 mmol, 0.3 ml). Change of color from green to violet was observed. The reaction progress was controlled by TLC ( $SiO_2$ ; acetone/hexane, 2:8). After 1 h the reaction was completed. The reaction mixture was quenched with water and the product was extracted with DCM (3 x 50 ml). The organic layer was washed with water (3 x 50 ml) The crude product was purified chromatographically by passing it through a short column filled with silica gel using a mixture of DCM/hexane 1:1 as the eluent. Yield: 193 mg (91 %), dark powder.  **$^1H$  NMR** (600 MHz,  $CDCl_3$ )  $\delta$ : 8.05 (d,  $J = 9.0$  Hz, 4H), 8.02 (d,  $J = 8.5$  Hz, 4H), 7.49 (d,  $J = 8.5$  Hz, 4H), 7.33 (dd,  $J = 8.3, 7.5$  Hz, 8H), 7.21 (d,  $J = 8.3$  Hz, 8H), 7.14 (t,  $J = 7.4$  Hz, 4H), 7.07 (d,  $J = 9.1$  Hz, 4H), 1.40 (s, 18H), the signal of the pyrrole ring protons overlaps with the doublet at 7.07 ppm (2H).  **$^{13}C$  NMR** (151 MHz,  $CDCl_3$ )  $\delta$ : 156.6, 152.3, 150.2, 146.7, 145.7, 142.2, 131.2, 130.2, 129.7, 129.2, 126.1, 125.6, 124.6, 124.1, 120.5, 118.0, 34.9, 31.4.  **$^{11}B$  NMR** (96 MHz,  $CDCl_3$ )  $\delta$ : 1.23 (t,  $J = 32.5$  Hz).  **$^{19}F$  NMR** (282 MHz,  $CDCl_3$ )  $\delta$ : - 111.01 (q,  $J = 32.8$  Hz). **UV-Vis** (THF)  $\lambda$  nm ( $\epsilon$  [ $M^{-1}cm^{-1}$ ]): 789 (83 000). **HR-ESI-MS**: calcd for  $C_{64}H_{56}N_5BF_2$  [M]: 943.4602. Found: 943.4602. **FT-ATR-IR**:  $\nu$  ( $cm^{-1}$ ) = 3058, 2956, 2865, 1584, 1467, 1427, 1406, 1331, 1271, 1194, 1132, 1087, 1030, 811, 750, 713, 692. **Anal.** Calcd for  $C_{64}H_{56}N_5BF_2$ : C, 81.40 %, H, 5.98 %, N, 7.42 %. Found: C, 81.14 %, H, 6.17 %, N, 7.06 %.

**Aza-BODIPY (7):** Aza-BODIPY **6** (0.15 g, 0.159 mmol) was dissolved in DCM (50 ml). In a separate flask N-bromosuccinimide (NBS, 28.3 mg, 0.159 mmol) was dissolved in DCM (25 ml). Both solutions were placed in an ice bath. The solution of NBS was added dropwise to the solution of **6** over a period of 2 hours. **Caution !:** it is imperative to maintain as slow addition of the cooled solution of NBS as possible to avoid any side reaction that could affect the purity of the final product. The solvent was removed on a rotary evaporator and the crude product was purified by a column chromatography (silica gel, acetone/hexane, 2:8

v/v). The product was dissolved in DCM (20 ml) and a methanol (20 ml) was slowly added. It was left to stand overnight for the DCM to evaporate. The amorphous precipitate was filtered and washed with methanol. Yield: 0.157 g, 96%. **<sup>1</sup>H NMR** (600 MHz, CDCl<sub>3</sub>) δ: 8.03 (d, *J* = 9.1 Hz, 2H), 8.00 (d, *J* = 8.5 Hz, 2H), 7.86 (d, *J* = 8.5 Hz, 2H), 7.72 (d, *J* = 8.8 Hz, 2H), 7.54 (d, *J* = 8.5 Hz, 2H), 7.40 (d, *J* = 8.5 Hz, 2H), 7.35 (dd, *J* = 8.4, 7.5 Hz, 4H), 7.31 (dd, *J* = 8.4, 7.4 Hz, 4H), 7.22 (t, *J* = 7.7 Hz, 8H, this signal is an overlap of two triplets each one with the integration equal 4H), 7.18 (t, *J* = 7.4 Hz, 2H), 7.14 (s, 1H), 7.10 (t, *J* = 7.4 Hz, 2H), 7.08 (d, *J* = 8.9 Hz, 2H), 7.02 (d, *J* = 9.1 Hz, 2H), 1.42 (s, 9H), 1.35 (s, 9H). **<sup>13</sup>C NMR** (151 MHz, CDCl<sub>3</sub>) δ: due to an overlap of signals we do not report <sup>13</sup>C NMR spectrum for this compound. **<sup>11</sup>B NMR** (96 MHz, CDCl<sub>3</sub>) δ: 0.81 (t, *J* = 31.4 Hz). **<sup>19</sup>F NMR** (282 MHz, CDCl<sub>3</sub>) δ: - 111.30 (q, *J* = 31.3 Hz). **FT-ATR-IR**:  $\nu$  (cm<sup>-1</sup>) = 3058, 2955, 2862, 1723, 1584, 1535, 1483, 1426, 1267, 1191, 1136, 1088, 1034, 814, 753, 714, 692. **UV-Vis** (THF)  $\lambda$  nm ( $\epsilon$  [M<sup>-1</sup>cm<sup>-1</sup>]): 769 (55 000). **HR-ESI-MS**: calcd for C<sub>64</sub>H<sub>55</sub>N<sub>5</sub>BF<sub>2</sub>Br: 1023.3701. Found: 1023.3702. **Anal.** Calcd for C<sub>64</sub>H<sub>55</sub>N<sub>5</sub>BF<sub>2</sub>Br: C, 75.12 %, H, 5.42 %, N, 6.85 %. Found: C, 74.29 %, H, 5.45 %, N, 6.36 %.

## 5. Conclusions

In conclusion, a synthesis of aza-BODIPY dye substituted with strongly electron-donating *p*-(diphenylamino)phenyl substituents (*p*-Ph<sub>2</sub>N-) at 3,5-positions was achieved through incorporation of boron difluoride (BF<sub>2</sub>-) into the corresponding aza-dipyrromethene ligand **5**. The latter was prepared via a four-step reaction: a Friedel-Crafts acylation of triphenylamine leading to ketone **2**, followed by formation of chalcone **3** via aldol condensation, followed by Michael addition of nitromethane to chalcone resulting in the corresponding 1,3-diaryl-4-nitro-butan-1-one **4**, followed by its conversion to aza-dipyrromethene **5**.

Both aza-BODIPY **6** and its mono-brominated derivative **7** exhibited a NIR absorption at  $\lambda_{\text{abs}}$  789 nm for **6** and  $\lambda_{\text{abs}}$  769 nm for **7** in THF, respectively. The compounds studied were very good absorbers of light and that was reflected in their relatively high molar extinction coefficients ranging from  $\epsilon = 48\,000\text{ M}^{-1}\text{cm}^{-1}$  to  $\epsilon = 83\,000\text{ M}^{-1}\text{cm}^{-1}$ . The crystallographic analysis of both aza-dipyrromethene **5** and its difluoroboron complex **6** revealed that the nitrogen atom of the *p*-Ph<sub>2</sub>N- groups adopted sp<sup>2</sup> hybridization facilitating the electron-donating effect of the diphenylamino group. We suggest, that it is probably the intramolecular charge transfer (ICT) nature of the excited state in **5-7** exerted by the

presence of strongly electron-donating *p*-Ph<sub>2</sub>N- groups that enhanced the non-radiative decay and was responsible for the lack of strong emission in these compounds. Upon excitation with  $\lambda_{\text{abs}}$  the compounds studied exhibited a negligible fluorescence with  $\Phi_f$  below 1 %. The combination of both nano- and femtosecond transient absorption techniques allowed detailed studies of ultrafast dynamics ( $\tau_s$  and  $\tau_T$ ) of *p*-Ph<sub>2</sub>N- substituted ADPM and aza-BODIPYs. Both compounds had very short-living excited singlet state lifetime of ca.  $\tau_s = 100$  ps. The excited triplet state lifetimes ( $\tau_T$ ) of the aza-BODIPYs in question equaled ca. 22  $\mu\text{s}$  at room temperature.

By incorporation of a heavy bromine atom into the structure of aza-BODIPY **6** we intended to induce a photosensitizing properties in this NIR photoactive compound. The mono-brominated derivative **7** proved to photosensitize oxidation of a model compound, viz. 1,3-diphenylisobenzofuran (DPBF), however, with relatively low quantum yield of  $\Phi_{\text{ox}}^{(\text{DPBF})} = 0.055$ . Interestingly, the photosensitized oxygenation of DPBF proceeded via Type I and/or Type III mechanism without formation and participation of singlet oxygen ( $^1\text{O}_2$ ).

CV and DPV measurements revealed that *p*-Ph<sub>2</sub>N- substituted ADPM and aza-BODIPYs underwent two irreversible oxidation and two irreversible reduction processes. The oxidation processes were observed at a very low oxidation potentials ( $E_{\text{ox}}^1$  from + 0.06 V to + 0.31 V) pointing to the very good electron-donating properties of these molecules. All compounds studied exhibited an outstanding photostability in THF solutions and very good thermal stability up to ca. 300 °C.

## 6. Acknowledgements

This work was supported by the NCN grant number DEC-2011/03/D/ST5/05910. The research was carried out with the equipment purchased thanks to the financial support of the European Regional Development Fund in the framework of the Polish Innovation Economy Operational Program (contract no. POIG.02.01.00-12-023/08).

## 7. References

- [1] J. Fabian, H. Nakazumi, M. Matsuoka, *Chem. Rev.* **1992**, *92*, 1197-1226.
- [2] G. Qian, Z. Y. Wang, *Chem. Asian J.* **2010**, *5*, 1006-1029.
- [3] J. V. Frangioni, *Curr. Opin. Chem. Biol.* **2003**, *7*, 626-634.
- [4] M. Z. Lin, *Nat. Methods* **2011**, *8*, 726-728.
- [5] S. Luo, E. Zhang, Y. Su, T. Cheng, C. Shi, *Biomaterials* **2011**, *32*, 7127-7138.
- [6] J. Zhao, W. Wu, J. Sun, S. Guo, *Chem. Soc. Rev.* **2013**, *42*, 5323-5351.
- [7] M. R. Detty, S. L. Gibson, S. J. Wagner, *J. Med. Chem.* **2004**, *47*, 3897-3915.
- [8] R. Bonnett, *Chem. Soc. Rev.* **1995**, *24*, 19-33.
- [9] K. M. Shafeekh, M. S. Soumya, M. A. Rahim, A. Abraham, S. Das, *Photochem. Photobiol.* **2014**, *90*, 585-595.
- [10] T. Yamagata, J. Kuwabara, T. Kanbara, *Heterocycles* **2014**, *89*, 1173-1181.
- [11] J. Schmitt, V. Heitz, S. Jenni, A. Sour, F. Bolze, B. Ventura, *Supramol. Chem.* **2017**, *29*, 769-775.
- [12] A. C. S. Lobo, A. D. Silva, V. A. Tomé, S. M. A. Pinto, E. F. F. Silva, M. J. F. Calvete, C. M. F. Gomes, M. M. Pereira, L. G. Arnaut, *J. Med. Chem.* **2016**, *59*, 4688-4696.
- [13] C. Shi, J. B. Wu, D. Pan, *J. Biomed. Opt.* **2016**, *21*, 050901-11.
- [14] J. L. Bricks, A. D. Kachkovskii, Y. L. Slominskii, A. O. Gerasov, S. V. Popov, *Dyes and Pigments* **2015**, *121*, 238-255.
- [15] C. Jiao, J. Wu, *Curr. Org. Chem.* **2010**, *14*, 2145-2168.
- [16] J. Zhao, K. Xu, W. Yang, Z. Wang, F. Zhong, *Chem. Soc. Rev.* **2015**, *44*, 8904-8939.
- [17] Y. Ge, D. F. O'Shea, *Chem. Soc. Rev.* **2016**, *45*, 3846-3864.

- [18] A. Gorman, J. Killoran, C. O'Shea, T. Kenna, W. M. Gallagher, D. F. O'Shea, *J. Am. Chem. Soc.* **2004**, *126*, 10619–10631.
- [19] M. J. Hall, A. O. McDonnell, J. Killoran, D. F. O'Shea, *J. Org. Chem.* **2005**, *70*, 5571-5578.
- [20] W. Zhao, E. M. Carreira, *Angew. Chem., Int. Ed.* **2005**, *44*, 1677-1679.
- [21] W. Zhao, E. M. Carreira, *Chem. Eur. J.* **2006**, *12*, 7254-7263.
- [22] V. F. Donyagina, S. Shimizu, N. Kobayashi, E. A. Lukyanets, *Tetrahedron Lett.* **2008**, *49*, 6152-6154.
- [23] R. Gresser, M. Hummert, H. Hartmann, K. Leo, M. Riede, *Chem. Eur. J.* **2011**, *17*, 2939-2947.
- [24] H. Lu, S. Shimizu, J. Mack, Z. Shen, N. Kobayashi, *Chem.–Asian J.* **2011**, *6*, 1026-1037.
- [25] M. Grossi, A. Palma, S. O. McDonnell, M. J. Hall, D. K. Rai, J. Muldoon, D. F. O'Shea, *J. Org. Chem.* **2012**, *77*, 9304-9312.
- [26] Y. Wu, C. Cheng, L. Jiao, C. Yu, S. Wang, Y. Wei, X. Mu, E. Hao, *Org. Lett.* **2014**, *16*, 748-751.
- [27] P. Majumdar, J. Mack, T. Nyokong, *RSC Adv.* **2015**, *5*, 78253-78258.
- [28] J. Killoran, L. Allen, J. F. Gallagher, W. M. Gallagher, D. F. O'Shea, *Chem. Commun.* **2002**, 1862-1863.
- [29] S. O. McDonnell, M. J. Hall, L. T. Allen, A. Byrne, W. M. Gallagher, D. F. O'Shea, *J. Am. Chem. Soc.* **2005**, *127*, 16360-16361.
- [30] W. M. Gallagher, L. T. Allen, C. O'Shea, T. Kenna, M. Hall, A. Gorman, J. Killoran, D. F. O'Shea, *Br. J. Cancer* **2005**, *92*, 1702–1710.
- [31] A. T. Byrne, A. E. O'Connor, M. Hall, J. Murtagh, K. O'Neill, K. M. Curran, K. Mongrain, J. A. Rousseau, R. Lecomte, S. McGee, J. J. Callanan, D. F. O'Shea, W. M. Gallagher, *Br. J. Cancer* **2009**, *101*, 1565–1573

- [32] D. O. Frimannsson, M. Grossi, J. Murtagh, F. Paradisi, D. F. O'Shea, *J. Med. Chem.* **2010**, *53*, 7337–7343.
- [33] N. Adarsh, R. R. Avirah, D. Ramaiah, *Org. Lett.* **2010**, *12*, 5720-5723.
- [34] R. Priefer, J. R. Griffiths, J. N. Ludwig, G. Skelhorne-Gross, R. S. Greene, *Lett. Org. Chem.* **2011**, *8*, 368-373.
- [35] P. Batat, M. Cantuel, G. Jonusauskas, L. Scarpantonio, A. Palma, D. F. O'Shea, N. D. McClenaghan, *J. Phys. Chem. A* **2011**, *115*, 14034–14039.
- [36] Y. Yan, J. Tian, F. Hu, X. Wang, Z. Shen, *RSC Adv.* **2016**, *6*, 113991-113996.
- [37] V. Ibrahimova, S. A. Denisov, K. Vanvarenberg, P. Verwilt, V. Pr eat, J-M. Guigner, N. D. McClenaghan, S. Lecommandoux, Ch-A. Fustin, *Nanoscale* **2017**, *9*, 11180-11186.
- [48] Q. Tang, W. Xiao, Ch. Huang, W. Si, J. Shao, W. Huang, P. Chen, Q. Zhang, X. Dong, *Chem. Mat.* **2017**, *29*, 5216-5224.
- [49] Q. Tang, W. Si, Ch. Huang, K. Ding, W. Huang, P. Chen, Q. Zhang, X. Dong, *J. Mater. Chem. B* **2017**, *5*, 1566-1573.
- [50] M. Strobl, A. Walcher, T. Mayr, I. Klimant, S. M. Borisov, *Anal. Chem.* **2017**, *89*, 2859-2865.
- [51] H.-J. Xiang, H. P. Tham, M. D. Nguyen, S. Z. F. Phua, W. Q. Lim, J.-G. Liu, Y. Zhao, *Chem. Commun.* **2017**, *53*, 5220-5223.
- [52] A. Coskun, M. D. Yilmaz, E. U. Akkaya, *Org. Lett.* **2007**, *9*, 607-609.
- [53] S. Liu, Z. Shi, W. Xu, H. Yang, N. Xi, X. Liu, Q. Zhao, W. Huang, *Dyes and Pigments* **2014**, *103*, 145-153.
- [54] X.-D. Jiang, J. Zhao, Q. Li, Ch.-L. Sun, J. Guan, G.-T. Sun, L.-J. Xiao, *Dyes and Pigments* **2016**, *125*, 136-141.
- [55] C. A. S. P, R. N. Priyanka, S. Mukherjee, P. Thilagar, *Eur. J. Chem.* **2015**, 2338-2344.

- [56] B. Zou, H. Liu, J. Mack, S. Wang, J. Tian, H. Lu, Z. Li, Z. Shen, *RSC Adv.* **2014**, *4*, 53864-53869.
- [57] N. Adarsh, M. S. Krishnan, D. Ramaiah, *Anal. Chem.* **2014**, *86*, 9335-9342.
- [58] S. Schutting, T. Jokic, M. Strobl, S. M. Borisov, D. de Beer, I. Klimant, *J. Mater. Chem C* **2015**, *3*, 5474-5483.
- [59] Y. Liu, J. Zhu, Y. Xu, Y. Qin, D. Jiang, *ACS Appl. Mater. Interfaces* **2015**, *7*, 11141-11145.
- [60] J. Killoran, S. O McDonnell, J. F. Gallagher, D. F. O'Shea, *New J. Chem.* **2008**, *32*, 483-489.
- [61] T. Li, T. Meyer, R. Meerheim, M. Höppner, C. Körner, K. Vandewal, O. Zeika, K. Leo, *J. Mater. Chem. A* **2017**, *5*, 10696-10703.
- [62] S. Kraner, J. Widmer, J. Benduhn, E. Hieckmann, T. Jageler-Hoheisel, S. Ullbrich, D. Schutze, K. S. Radke, G. Cuniberti, F. Ortmann, M. Lorenz-Rothe, R. Meerheim, D. Spoltore, K. Vandewal, C. Koerner, K. Leo, *Phys. Status Solidi A* **2015**, *212*, 2747-2753.
- [63] S. Y. Leblebici, L. Catane, D. E. Barclay, T. Olson, T. L. Chen, B. Ma, *ACS Appl. Mater. Interfaces* **2011**, *3*, 4469-4474.
- [64] M. Frenette, M. Hatamimoslehabadi, S. Bellinger-Buckley, S. Laoui, S. Bag, O. Dantiste, J. Rochford, C. Yelleswarapu, *Chem. Phys. Lett.* **2014**, *608*, 303-307.
- [65] R. Gresser, H. Hartmann, M. Wrackmeyer, K. Leo, M. Riede, *Tetrahedron* **2011**, *67*, 7148-7155.
- [66] A. Loudet, R. Bandichhor, L. Wu, K. Burgess, *Tetrahedron* **2008**, *64*, 3642-3654.
- [67] A. Loudet, R. Bandichhor, K. Burgess, A. Palma, S. O. McDonnell, M. J. Hall, D. F. O'Shea, *Org. Lett.* **2008**, *10*, 4771-4774.
- [68] Ł. Łapok, M. Obłozza, A. Gorski, V. Knyukshto, T. Raichyonok, J. Waluk, M. Nowakowska, *ChemPhysChem* **2016**, *17*, 1123-1135.
- [69] A. Gut, Ł. Łapok, D. Drelinkiewicz, T. Pędziński, B. Marciniak, M. Nowakowska, *Chem. Asian J.* **2018**, *13*, 55-65.

- [70] M. Obłozza, Ł. Łapok, J. SolarSKI, A. Gorski, T. Pędziński, M. Nowakowska, *Chem. Eur. J.* **2018**, *24*, 7080-7090.
- [71] M. Obłozza, Ł. Łapok, T. Pędziński, K. M. Stadnicka, M. Nowakowska, *ChemPhysChem* **2019**, *20*, 2482-2497.
- [72] A. Gut, Ł. Łapok, D. Jamróz, M. Nowakowska, *Asian J. Org. Chem.* **2017**, *6*, 207-223.
- [73] D. Patil, M. Jadhav, K. Avhad, T. H. Chowdhury, A. Islam, I. Bedja, N. Sekar, *New J. Chem.* **2018**, *42*, 11555-11564.
- [74] Ł. Łapok, M. Cyza, A. Gut, M. Kępczyński, G. Szewczyk, T. Sarna, M. Nowakowska, *J. Photochem. Photobiol. A* **2014**, *286*, 55-63.
- [75] P. Carloni, L. Damiani, L. Greci, P. Stipa, F. Tanfani, E. Tartaglini, M. Wozniak, *Res. Chem. Intermed.* **1993**, *19*, 395-405.
- [76] S. E. Braslavski, „*Glossary of terms used in photochemistry.*”, 3rd edition, **2006**, UPAC recommendation 2006.
- [77] C. M. Cardona, W. Li, A. E. Kaifer, D. Stockdale, G. C. Bazan, *Adv. Mater.* **2011**, *23*, 2367-2371.
- [78] P. Bujak, I. Kulszewicz-Bajer, M. Zagorska, V. Maurel, I. Wielgus, A. Proń, *Chem. Soc. Rev.* **2013**, *42*, 8895-8999.
- [79] A. Gut, Ł. Łapok, D. Jamróz, A. Gorski, J. SolarSKI, M. Nowakowska, *New J. Chem.* **2017**, *41*, 12110-12122.
- [80] M. Obłozza, Ł. Łapok, T. Pędziński, M. Nowakowska, *Asian J. Org. Chem.* **2019**, *8*, 1879-1892.